STUDY OF SOME PARAMETERS OF INMOLD PROCESS FOR NODULAR CAST IRON PRODUCTION USING A NICKEL COATED MAGNESIUM POWDER

By

SANJEEV BHARGAVA

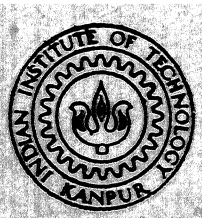

DEPARTMENT OF METALLURGICAL ENGINEERING

INDIAN INSTITUTE OF TECHNOLOGY KANPUR

JANUARY, 1978

STUDY OF SOME PARAMETERS OF INMOLD PROCESS FOR NODULAR CAST IRON PRODUCTION USING A NICKEL COATED MAGNESIUM POWDER

A Thesis Submitted
In Partial Fulfilment of the Requirements
for the Degree of
MASTER OF TECHNOLOGY

By
SANJEEV BHARGAVA

to the

DEPARTMENT OF METALLURGICAL ENGINEERING
INDIAN INSTITUTE OF TECHNOLOGY KANPUR

JANUARY, 1978

C E R T I F I C A T E

It is certified that the work entitled "Study of some parameters of Inmold Process for nodular cast iron production using a nickel coated magnesium powder" has been carried out under my supervision and that this has not been submitted elsewhere for a degree .

V Bansal

Date : January 6, 1978

V. Bansal
Assistant Professor
Department of Metallurgica
Engineering.
Indian Institute of Techno
KANPUR-208016, U.P., India.

ACKNOWLEDGEMENTS

I am indebted to Dr. V. Bansal, Assistant Professor, Department of Metallurgical Engineering, for his valuable suggestions and constant inspiration in course of this work.

Friendly appreciation is also expressed to those who helped me in many ways, direct or indirect.

B. BHARGAVA

LIST OF FIGURES AND MICROGRAPHS

NOMENCLATURE

A	Area of the alloy chamber
2a	Width of the runner ingate to the alloy chamber.
2b	Diameter of the sprue base
C	Concentration of magnesium dissolved in the liquid stream.
C*	Required dissolution of magnesium in the liquid stream which will give full nodularization.
D	Diameter of the alloy chamber
d	Particle size of the inoculant kept in the alloy chamber.
f	Solution factor.
g	Acceleration due to gravity.
H	Height of the downsprue.
h	Deapth of the alloy chamber.
K_1	Coefficient defined by equation (II.14).
K_2	Coefficient defined by equation (II.15).
R	Radius of the magnesium-nickel composite powder.
r	Radius of the core magnesium particle .
T	Temperature
t	Thickness of the nickel shell over magnesium particle.
v	Velocity of the liquid metal stream over the alloy chamber.

W_{Ti}, W_{Pb}, etc.	Weight percentage of the subscripted element.
x	Length of the alloy chamber along the liquid flow.
ρ_{Ni}	Density of nickel.
ρ_{Mg}	Density of magnesium.
ACC	Area-Concentration-Curve.
AVC	Area-Velocity-Curve.
CEV	Carbon Equivalent value
VG	Vermicular Graphite.

ABSTRACT

The uniform dissolution of the treatment alloy in the inmold process requires the knowledge of its "Solution factor" which is the optimum ratio between liquid metal stream velocity and the alloy chamber area. The present study involved the finding of solution factor of nickel coated magnesium powder which was dissolved in the liquid cast iron stream of composition, C-3.9%, Si-2.58%, S-0.009% and p-0.11% The composite powder was prepared by electroless plating of nickel on magnesium and contained 11.9% nickel. Velocity of the liquid metal stream over the alloy chamber area was kept constant at an average value of 25 cm/sec. and the area of the chamber was varied from 20 cm^2 to 62 cm^2. The biggest area alloy chamber provided a magnesium dissolution of 0.032% in the melt and gave rise to the vermicular graphite in cast iron. Lower magnesium dissolution gave either vermicular graphite or flake graphite. Solution factor was determined by extrapolating the experimentally obtained plot between the magnesium dissolution and the alloy chamber area. At the pouring temperature of 1350 ^{o}C the solution factor was found to be 0.2 cm^{-1} sec^{-1}.

Desulphurization of cast iron was carried out using -200 mesh size calcium carbide powder which was mixed in the

melt using a fire clay stirrer of a simple shape. Within five minutes after calcium carbide addition the sulphur reduced to 0.009% amounting to approximately 70% sulphur removal.

—

CHAPTER I

I.01 INTRODUCTION :

The quantity and form of graphite in cast irons exert a major influence on its properties, and since both of these can be controlled by inoculants added into the liquid melt, inoculation treatment becomes the decisive factor for the production of high quality cast irons. Inoculants are added to the liquid melt in small quantities ($< 0.3\%$) and the purpose is to change the morphology of the solidifying phase rather than changing the chemical composition. While ferro-silicon, calcium silicide, aluminium, graphite and zirconium have been reported to work as inoculants for flake graphite cast iron, nodular graphite cast iron is obtained by inoculating liquid melt with magnesium, cerium, calcium, lithium, sodium or rare earths. Yamamoto et al[1] suggest that H_2, N_2, CO_2 and Ar also can act as graphite nodularizers. Gorshkov[2] used CH_4 to produce graphite nodules in cast iron.

Nodular cast iron was first produced in 1948 by Morrogh and Williams[3] and can be rightly called an epoch making discovery because it is a material which combines some of the most desirable engineering properties of materials. It possesses excellent ductility, good toughness, good machinability while retaining all inherent characteristics of grey cast iron such as excellent castability, excellent

damping capacity and good wear and corrosion resistance. Its world production has already exceeded two million tons per year and is expected to reach twenty million tons eventually[4].

I.02 MORPHOLOGY OF GRAPHITE IN CAST IRONS :

As its name suggests nodular cast iron consists of graphite nodules embedded in a matrix which may be ferritic, pearlitic or martensitic. Morrogh[5] points out that nodules are not merely balls of graphite but are an aggregate of crystallites growing outward from a common nucleus, close packed planes (0001) being at right angles to the radial direction of the spheroid (see Figure I.1). This particular arrangement of crystallites forming nodular structure is called spherulite and hence the nodular cast iron as the spheroidal graphite, spherulitic graphite and in short SG iron. Since the ductility of nodular cast iron is much more than that of gray cast iron it is also called ductile cast iron.

In contrast with the spherulitic shape of graphite which exists in nodular cast iron, flakes in gray cast iron grow along the poles of the prism planes which are in contact with the melt to produce interconnected flakes[6]. These flakes may be large or small, straight or curled but always have a very high length to thickness ratio .

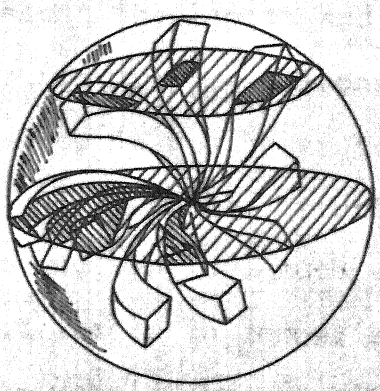

Fig. I. 1a. Schematic represention of graphite crystallites nucleating from a common centre in nodular iron. (Ref. 5)

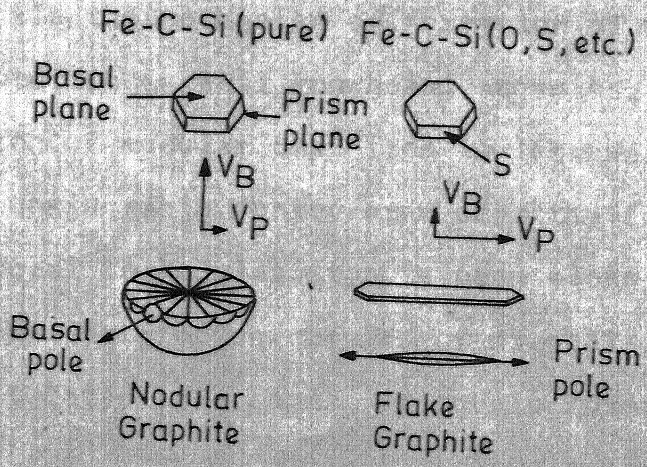

Fig. I. 1b. Graphite growth morphologies for nodular and flake graphite. (Ref. 6)

If 'l' and 'g' represent the length and thickness of the flake then generally for gray cast irons $(l/g) > 50$[11].

At this point, it can be stated that this ratio for nodular graphite will be one. Structures where this ratio is between two and ten i.e. much smaller than that of flake graphite but larger in comparison to spherulitic graphite are known as vermicular graphite cast irons or VG cast irons[7 - 10].

The study of vermicular graphite is still rather recent and can be found in the specialized literature under various names such as : type "P" graphite, "P441" graphite, Form III, pseudo-lamellar, chunky graphite and melkoplastinatyjgrafit[11]

While the mechanism of formation of flake graphite-austenite eutectic is well known and accepted, the eutectic solidification of modular cast iron is less well understood. There is a considerable controversy over the forces that cause the nuclei in nodular iron to grow along the pole of the basal plane to produce nodules of graphite. Among the theories postulated to account for nodule formation are the following[6]:

(1) Graphite nodules form as a result of an attempt of the melt to minimize its free energy by minimizing graphite-melt interfacial area.

(2) Nodule formation depends on the absence of certain surface-active elements which alter the growth direction of graphite from the pole of the basal plane to the pole of the prism plane.

(3) Nodule growth depends on surface adsorption of the nodularizing addition onto the graphite lattice which causes a change in the growth direction from the pole of the prism plane to the pole of the basal plane.

(4) Graphite nodules grow within an austenitic shell or from supersaturated austenite.

(5) The graphite growth direction depends on the type of nuclei upon which growth is initiated.

(6) Graphite nodules form in gas bubbles within the melt.

(7) Nodules form as a consequence of non-equilibrium growth associated with undercooling.

I.03 PRODUCTION OF NODULAR CAST IRON - PROBLEMS ASSOCIATED WITH :

Role of an inoculant has already been discussed. The following requirements emerge for graphite nodularizing materials/alloys[4] :

(1) the treatment must be simple and safe

(2) the media must dissolve and distribute in the melt properly

(3) they should set up movements in the bath to produce a kind of self cleaning action although this can be

achieved by mechanical means too.

Although the above requirements are satisfied by all nodularizers mentioned in the earlier section (also see Table II.2) it is the magnesium process which has been accepted for commercial production of nodular cast iron because it satisfies them both technically and economically. It has predominated over cerium process mainly because it can be applied to a wider composition of base iron, the cerium being applicable to irons of hyper-eutectic analysis only.

The simplest way to produce nodular cast iron, therefore, would be to add pure magnesium in its metallic form. But it would require a complicated process technology because magnesium vapourizes at 1107°C i.e. at temperature below which cast irons melt and has a very high vapour pressure of 6 to 10 atmospheres at the corresponding treatment temperatures of 1400°C and 1500°C. As a result, the magnesium vapourizes on contact with the molten iron, and the reaction may be quite violent if it is not carriedout properly. Also, its density being lower than that of the liquid cast iron, it tries to float at the top and as soon as it reaches the surface it reacts with atmospheric oxygen to form oxide and for all practical purposes the melt remains untreated. Moreover, when put in the cast iron, it combines first with the sulphur and oxygen present in the cast iron and gets

used up by them. Khropov and Bedarev[36] investigated that the sulphur reduction, because of magnesium sulphide formation, was 74-92% during the holding period and fell most rapidly over the first 10-20 min. About 45% loss of magnesium occurred during the first 20 min. mainly due to desulphurization. They also reported that due to volatilization of magnesium which continuously takes place if the inoculated melt is held for some time graphite content of the casting also decreases . Loss of magnesium as vapour ceases when the temperature falls to 1107°C. Thus the active portion of magnesium in the liquid melt is obtained only for a limited time. This continuous lowering of concentration of active magnesium in the melt with time is known as fading. White[37] suggests that 0.01% magnesium is lost every 10 min during which a ladle of treated metal stands at 1480°C. These problems associated with the dissolution of magnesium in the melt and its subsequent fading give rise to a poor magnesium recovery.

In order to maximize the recovery of magnesium and to make the treatment process simple, various magnesium alloys have been developed and successfully used for nodular iron production. While alloying elements improve the mechanical properties they also reduce the volatility of magnesium at the treatment temperature.

Recovery is also dependent on the treatment process and thus, in principle, can be improved by developing better process. Conventional methods for magnesium treatment are many[4] and a maximum of 40-50% alloy recovery has been obtained by some of them. While there are possibilities that in future a better magnesium recovery will be obtained by modifying conventional processes, there is doubt whether they will be able to provide answers to problems of the fading phenomenon, pigging of the heat if there is a sudden power failure in the plant, complete automation of the foundry plant and lastly uniform nodule count/mm^2 and their distribution in different castings poured from the same heat. Inmold process is the latest method of inoculation and answers most of these questions.

In the inmold process, a chamber of suitable dimensions is formed within the mold pouring system. The nodularizing alloy is placed in this chamber in such a way that a controlled reaction occurs at a uniform rate until the mold is filled without contamination from any residual slag inclusions. Due to the fact that the alloy metal reaction takes place in the relative absence of air there are no fumes or pyrotechnics and the alloy recovery, which in turn depends on the type of alloy, is very high; upto 80% or more. Also the improved nucleation reduces the tendency for carbide formation particularly in thin section castings.

CHAPTER II

REVIEW OF THE LITERATURE

II.1.01 INMOLD PROCESS :

Since the effectiveness of the treatment alloy is found to be maximum when the time between its addition and the beginning of the solidification is the shortest, it can be maximised by introducing the treatment alloy directly inside the mold or in the gate, runner or cavity upstream of the casting ingate. However, for such a process to be successful, the following fundamental requirements have to be satisfied[13,15] :

(1) A supply of hot clean molten iron of the required specification.

(2) A treatment alloy which promptly dissolves in the liquid melt at the treatment temperature.

(3) A stream of molten metal coming in contact with the inoculant in such a manner that a controlled reaction occurs at a uniform rate until the mold is filled.

(4) Undissolved alloy residues must not be allowed to be dragged inside the casting.

While first two requirements pose material problems, later two, which are not readily compatible, have to be solved by properly designing the mold and have to be exclusively determined for pre-selected molten iron and the inoculant.

Various solutions have been proposed depending both on the point where the alloy must be added and on the alloy's most suitable shape i.e. a single piece or loose granules or, still, granule compact specially shaped as necessary[12-24].

Dunks,[14] McCaulay[15], and Remondino et al[16,17] have given a solution which seems to be the most attractive from the point of view of the uniform dissolution of nodularizing alloy. It consists in placing the alloy, in the powder form, in a chamber suitably shaped to maintain the solution rate practically constant during pouring provided that the iron flow rate is always the same. An example of a very simple chamber design is shown in Figure-II.1 . Effectiveness of this simple alloy chamber can be understood in terms of the "solution Factor" which is part of the discussion of the next section.

II.1.02 CONCEPT OF THE "SOLUTION FACTOR" :

Let us visualise a situation in which a liquid is flowing through a tube with a velocity 'V' and in the way it encounters with solid particles kept in a chamber shown in Figure II.1 . These solid particles are readily soluble in the liquid. In our case, liquid, tube and solid particles correspond to liquid cast iron, runner system and inoculant powder respectively.

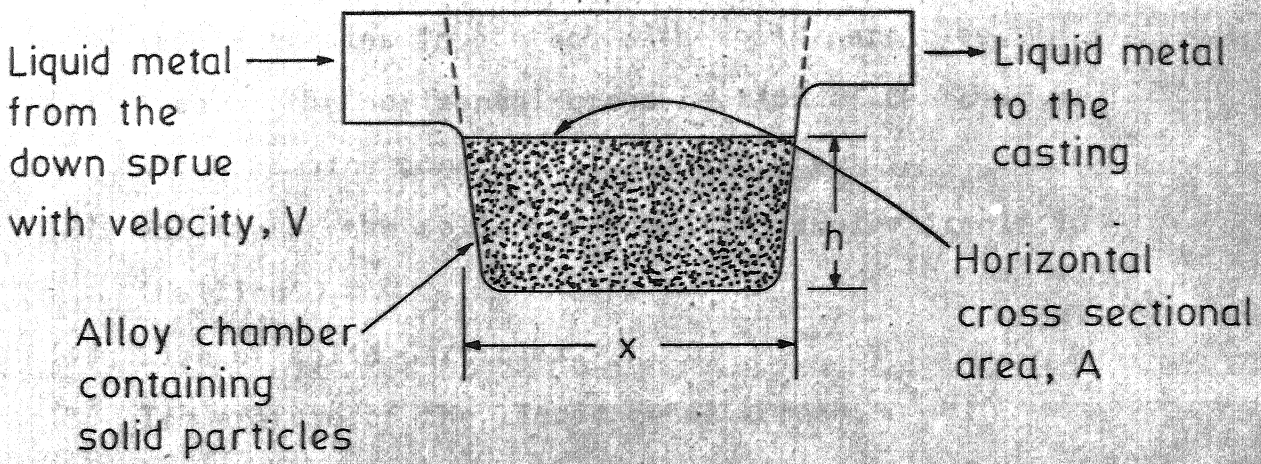

Fig. II.1. The alloy chamber for the treatment inside the mould.

As soon as the flowing liquid comes in contact with these particles it starts dissolving them. The amount of dissolved solid due to its pick up in the stream, will depend on the following factors :

(1) Time during which a particular volume element of the liquid remains in contact with solid particles.

(2) Area of the horizontal cross section of the chamber, witch remains constant at all heights.

(3) Ability of the solid to promptly dissolve itself in the liquid.

(4) Size of solid particles.

(5) Temperature of the liquid metal stream.

It can be seen from abovementioned requirements that while the alloy solubility and effect of particle size can be learnt from either complicated theories or a shear experience, effects of time, horizontal cross sectional area of the chamber and the temperature of the metal stream can be easily predicted.

(1) Time :

Assume the length of the chamber along the liquid flow direction to be 'X' . Then the time during which a particular volume element of liquid melt will remain in contact with solid particles will be (X/V) units of time . Thus, it can be said that a rapidly flowing liquid will remain in contact with solid particles for a shorter time

and vice versa. Hence the dissolution rate will be inversely proportional to the velocity.

(2) Horizontal Area of Cross Section of the Alloy Chamber :

Bigger cross sectional area of the chamber means that more particles come in contact with the flowing metal. Hence the dissolution rate will be proportional to the chamber cross sectional area and a linear relationship between them would be expected.

(3) Temperature :

Dissolution rate of solid particles will be more at higher temperatures .

The effect of particle size is quite complicated because it would require the knowledge of shape, wetting ability and density of the solid. However, it can be assumed that the dissolution will be an inverse function of the particle size, d.

Therefore if 'C' iw the concentration of solid particles in the liquid melt then

$$C = F_1 \left[(1/v),\ A,\ T,\ f\ (1/d) \right] \qquad (II.1)$$

Or, if the system is studied at a fixed temperature for a particular size particles, the equation (II.1), in its simplified form, can be written as

$$C = F_2 \left[(1/v), A \right] \qquad (II.2)$$

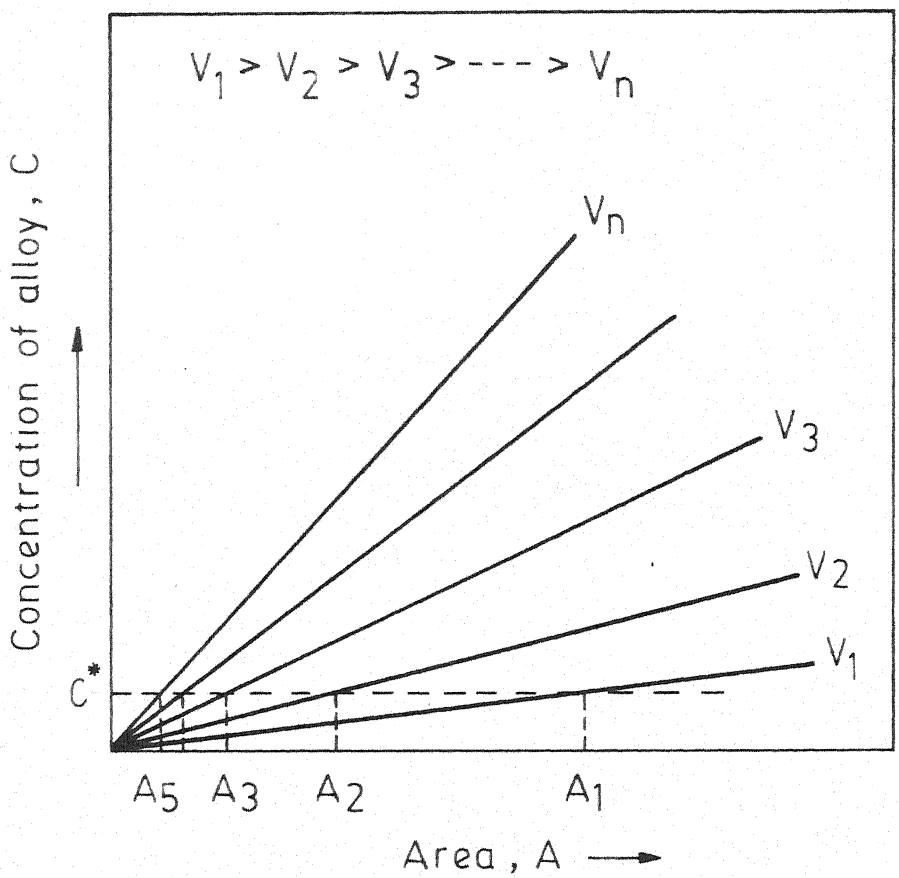

Fig. II.2. Area - concentration curves (ACC)

Equation (II.2) suggests that one can plot the effect of horizontal cross sectional area of the alloy chamber on the concentration of solid . Keeping the velocity constant. Area-concentration-curves (ACC) for different velocities are shown in Figure-II.2 . Utility of ACC can be judged from the following arguments .

Suppose C* is the most desirable concentration of the solid in the liquid melt. Then ACC show that C* can be obtained by a set of areas and velocities as shown in Figure-II.2 . Using these values i.e. A_1 , A_2, A_3 .....A_n and V_1 , V_2 , V_3 .... V_n , one can plot a relationship between them.

McCaulay[15] suggests that the relationship between velocity and area, i.e. velocity-Area-curve (VAC) is linear as shown in Figure II.3 . The shape of VAC is often called the "Solution Factor", "Solubility Factor" or sometimes "Solution Reactivity Factor" .

Therefore

$$\text{Solution Factor , } f = \frac{\text{Velocity}}{\text{Area}} \qquad \text{(II.3)}$$

As shown in Figure- II.3, the solution factor, f, can be influenced by temperature and one would expect a lower f at higher temperatures. McCaulay[15] points out that for cast irons practically no significant variation in f is

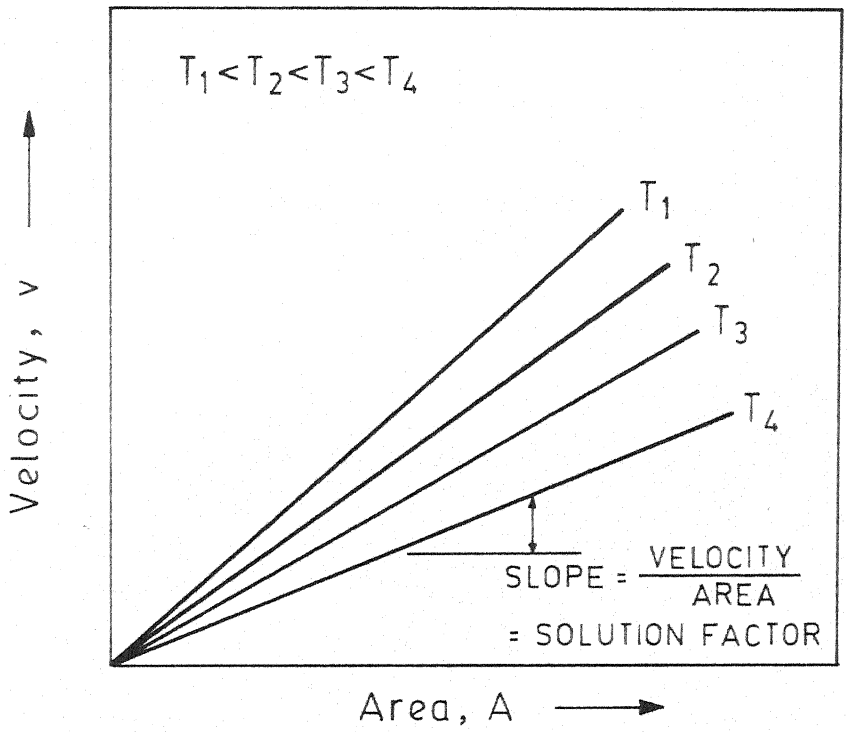

Fig. II.3. Velocity - Area - curves (VAC)

observed within a temperature range of $\pm 40^{\circ}C$.

It is interesting to note that the solution factor is independent of the casting weight which in turn determines the total amount of the inoculant required. Thus if the solution factor is determined for a particular alloy and a particular shape of the alloy chamber it can serve as a useful guideline for all castings to be inoculated by that particular alloy. The designer then only varies the alloy chamber depth for castings of different weights for providing the required amount of the alloy and assures a uniform alloy dissolution throughout pouring. As can be seen from Figure- II.4 [19] the dissolution of the alloy is uniform and provides a consistent magnesium level in all parts of the casting.

A careful look over figure II.4(a) will reveal that our previous conclusion that the solution factor will remain unchanged by a vertical dimensioning of the alloy chamber is not strictly true. The drop in height h in time t will increase the velocity of the melt by

$$v = \sqrt{2g}\left(\sqrt{h_2} - \sqrt{h_1}\right) \qquad \text{(II.4)}$$

where

$$\Delta h = h_2 - h_1$$

but for all practical purposes it can be assumed that and thus solution factor remains constant.

With this much information of the solution factor, demerits of "a single piece inoculant method"[16,21] can be

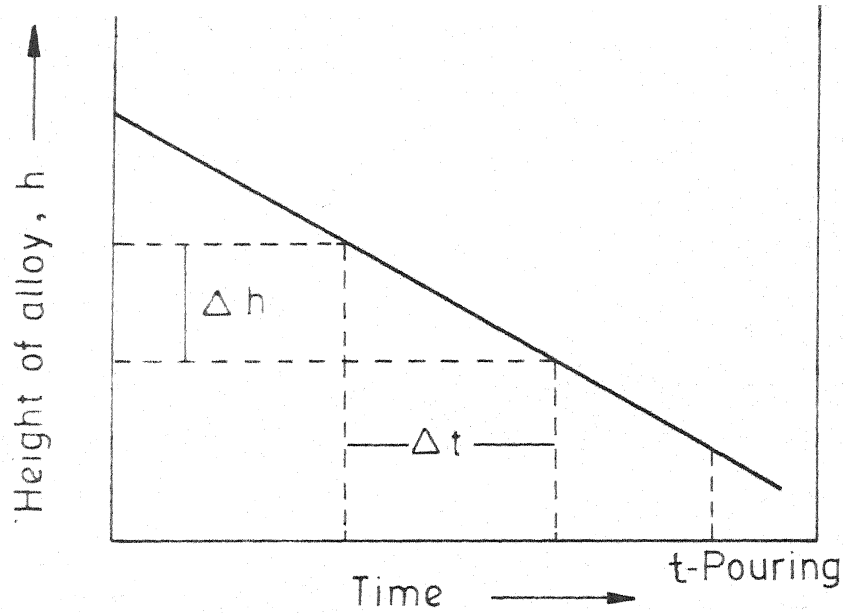

(a)

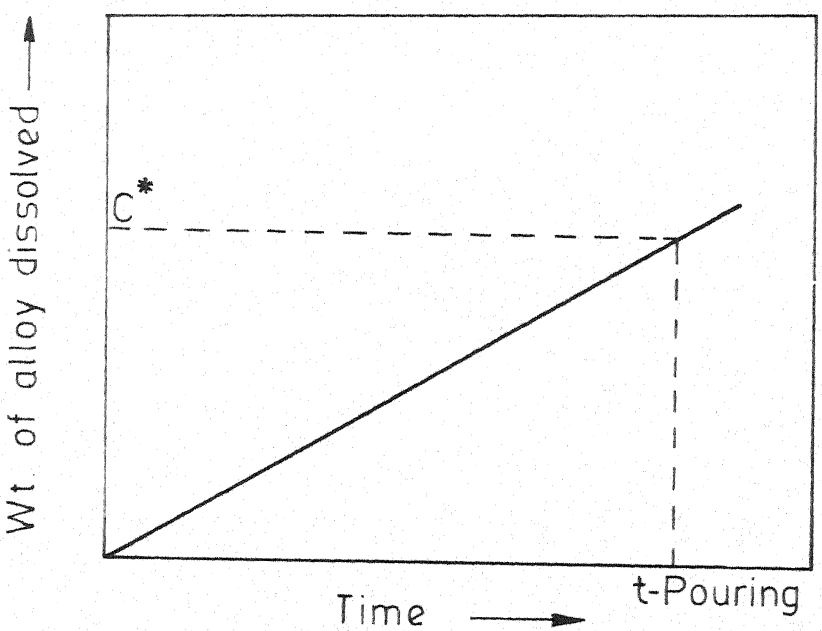

Fig. II.4. Dissolution of alloy from the alloy chamber[19]

realised as it is nonconsistent in dissolving the inoculant in different phases of casting[13]. Actually the alloy mass is cold at first and then heats up rapidly. The dissolution rate rises then quickly upto a maximum value and afterwards decreases because the alloy mass surface also decreases rapidly increasing the solution factor. This trouble can actually be reduced either by iron stirring which may occur in rather large castings or through certain expedients such as suitably shaping the alloy masses. These provisions are, however, costly and effective only if specifically developed for each casting[12].

II.1.03 INCLUSIONS IN INMOLD CASTINGS:

Inmold castings have been reported[13,15,17] to contain unwanted inclusions which are trapped in the casting because of the inherent characteristics of the inmold process.

If the alloy chamber is not properly designed the metal stream flowing over alloy might create a violent turbulance leading to both grain displacements and projections. The projected areas further increase the turbulance and at one stage chip off to be dragged in the actual casting by the quickly solidifying metal. If these particles are big and cannot be dissolved completely before the metal solidifies, they will form inclusions. This problem, however, can be reduced by keeping smaller particles in the alloy chamber. Thus the problem of inclusions sets the upper limit of particle size to be kept in the alloying chamber. This limit

will be different for different alloys and in general will depend on the pouring temperature.

If pouring is uninterrupted, the metal has a high fluid pressure and a head of metal is always kept at the alloy chamber the dissolution of the alloy and its reaction with the liquid stream takes place almost in the absence of air and the casting is expected to be clean unless the liquid metal itself contains impurities . However, the above statement is not true for the very first element of the liquid stream because alloy dissolution in it does take place in the presence of air. Because of being the first element of metal to enter the mold it also carries away dross and slag formed by the turbulance created in the pouring basin and vertical sprue. Therefore, to keep this element of metal from getting into the casting cavity, where it will cause inclusion edefects, it must be retained in the runner cavity. The gates should be placed along the side of the runner so that the first iron flows past them. Flow through the gates commences only after the end of the runner stops the flow and the level of liquid iron rises in the runner. In other words, the runner should include an extension past the last gate to trap the slag in the initial melt. By the time the gates become operative, the liquid level in the runner must be above the top of the gates. Then no slags can enter the casting cavity. A thin, wide gate connected to a tall narrow

runner will facilitate the action. Moreover, the runner must be large enough in cross section and long enough to permit the slag to float to the surface of the metal and adhere to the top of the runner[25].

Moore[17] suggests that slag-inclusions can be eliminated by using a dam-type skimmer and choking just beyond the dam. He suggests that the dam itself represents a convenient place to put the alloy providing that the total amount of alloy used does not occupy more than half the volume of the dam area. Too much alloy could very easily stop the initial flow of metal to the casting and cause a misrun. Polystyrene passages can be used to control the flow of metal through the alloy in defined manner, but these are not normally necessary. Polystyrene is also a useful material to temporarily slow down flow rate at the dam gate exit so slag and dross can float above the dam to exit in the initial stages of pour.

II.1.04 DESIGN OF THE ALLOY CHAMBER :

Disadvantages of having a turbulent iron flow over the alloy chamber have been pointed out in the earlier section. Askeland, Trojan and Flinn[26] point out that turbulent flow breaks up the fluid dross film producing stringers and gross dross defects in the castings. Increased turbulance also permits reaction between dissolved magnesium and air in the unfilled casting to produce the fine MgO dross defect.

Smooth metal flow is necessary not only for clean castings but also for uniform alloy dissolution in the liquid melt. Turbulance may, sometimes also generate vortexes and dead corners where the dissolution is stronoly slowed or even incomplete .

Remondino et al[13] suggest that in general care should be taken to avoid iron entering the chamber with an excessive difference of level, more than 20 mm (3/4 in.) Furthermore it is preferable to widen the section of the entrance and to locate the exit at a higher level than that of the entrance, sometimes with an outlet on the chamber ceiling. The exit zsection must be at least 10% smaller than that of the entrance. The effect of choking facilitates alloys dissolution in both initial and subsequent phases.

II.2.01 ALLOY SELECTION FOR INMOLD PROCESS :

For inoculation treatment inside the mold the alloy must have specific characteristics. In fact, resistance to fading is no longer important. The dissolution rate in the iron flow is now the governing factor. Thus, an alloy which is effective when used in the ladle may prove unfit inside the mold if its discolution rate in the iron is too low (inoculation in the first part of the casting is insufficient) or too high (inoculation in the last part of the casting is insufficient). In addition to the dissolution rate, analysis

and grain size of the alloy should be uniform . Any irregularities in the composition or impurities present can not be tolerated because the small amount of alloy added to the mold will no longer be diluted as in a big batch, therefore the castings will undergo poor inoculation and will contain inclusions. In fact, the concept of uniformity of composition and grain size distribution can no longer be applied to the average sample from an alloy drum or a carload but must now be referred to small amounts as the ones intended for the suitable chambers in the molds e.g. 20 to 100 gms, This requirement is slightly difficult to follow by conventional alloy producers mainly because of a very high degree of segregation involved during these alloy's solidification.

Although high magnesium alloys are not used by conventional nodular iron making processes, Moore[17] points out that inmold process can utilise them without causing any pyrotechnic fumes and with an increased effectiveness and recovery.

Rao and Tamhankar,[26] and Kaul[27] have coated various powders with nickel using electroless plating. Their methods give a uniform coating of nickel over the parent powder giving us a powder composite. If such a nickel coated magnesium powder can be developed then it will fulfill requirements of uniformity of both, chemical composition as well as the particle size distribution of the inoculation alloy. Since

the magnesium is supposed to be as high as 90% in the composite powder, its recovery is also expected to be better.

II.2.02 ELECTROLESS PLATING OF NICKEL ON MAGNESIUM :

In electroless plating a suitable buffer solution of the element to be coated is mixed with a reducing solution. These solutions then interact to cause the controlled precipitation of the "metal plating". Plating of nickel involves the deposition of nickel by hypophosphite as follows[27] :

$$(H_2PO_2)^- \xrightarrow{\text{catalyst}} (PO_2)^- + 2H\ (\text{catalyst}) \qquad (II.6)$$

$$(PO_2)^- + H_2O \longrightarrow H^+ + (HPO_3)^{2-} \qquad (II.7)$$

$$Ni^{++} + 2H(\text{Catalyst}) \longrightarrow Ni + 2H^+ \qquad (II.8)$$

$$(H_2PO_2)^- + H(\text{catalyst}) \longrightarrow H_2O + OH^- + P \qquad (II.9)$$

$$2H(\text{catalyst}) \longrightarrow H_2 \qquad (II.10)$$

Reaction (II.6) states that hypophosphite anions are dehydrogenated catalytically to metaphosphite ions. The abstracted hydrogen, either in the atomic or in any "activated" form is adsorbed on the catalyst which could be, at that stage, considered a "hydride" in the broadest sense

Reaction (II.7) states that the metaphosphite ion reacts with water to form orthophosphite anion. It should be noted that this reaction implicitly indicates the formation of hydrogen ions, which explains the pH dependency of reactions

(II.6) and (II.7) . Reactions (II.6) and (II.7) are, of course, simultaneous.

Reaction (II.8) represents the reduction of nickel ions to metallic nickel by active hydrogen atoms adsorbed on the catalytic surface, with formation of hydrogen cations.

Reaction (II.9) represents symbolically the dehydration-reduction of hypophosphite to active phosphorus, which combines with nickel to form a nickel-phosphorus alloy.

Reaction (II.10) represents the formation of molecular (gaseous) hydrogen.

It can be seen that reactions (II.6) and (II.7) (togather) are favoured by a high pH value. This is also true for reaction (II.8) because hydrogen ions are formed on the right side. On the other hand, reaction (II.9) must be slowed down by a high pH (low hydrogen ion concentration) as one of its products is the hydroxyl $(OH)^-$ ion.

In acid solutions, there is a further reaction to be considered :

$$Ni + 2H^+ \longrightarrow Ni^{2+} + H_2 \qquad (II.11)$$

This reaction expresses the fact that the deposited nickel is dissolved, with evolution of hydrogen gas, when the pH is sufficiently low.

The catalyst must be an active dehydrogenation agent as clear from the reaction (II.6), for this reaction to proceed in the forward direction. Numerous metals e.g. iron,

aluminium, copper, gold, silver etc. have been called "catalytic" for this reaction.

Considering reaction (II.8) it can be seen that, in a batch operation the solution will become more and more acidic as the reaction proceeds, until the rate of reaction (II.11) becomes equal to that of the nickel alloy deposition , and the latter will eventually stop. In order to allow the deposition reaction to proceed continuously or to completion, it is necessary to keep the pH substantially constant. This can be achieved by periodic or continuous addition of a neutralizing chemical, i.e. of hydroxyl ions. It can also be promoted by incorporating a buffer in the bath composition (like citric or malic anions).

Table II.1 gives the composition of two suggested[28] acid baths :

Table II.1 Conditions For Electroless Plating In Acid Bath

Components/conditions	concentration g/L	
	Bath No. 1	Bath No. 2
Nickel chloride	30	-
Nickel sulphate	-	30
Sodium Acetate	-	10
Sodium Citrate	10	-
Sodium hypophosphite	10	10
pH range	4 - 6	4 - 6
Temperature	90 °C	90 °C
Rate of plating mils/hr	0.2	1

II.2.03 PROPOSED MECHANISM FOR NODULARIZATION BY NICKEL COATED MAGNESIUM POWDER :

Assuming core particles of magnesium to be spherical and coating of nickel to be uniform, the shell thickness 't' is given by, (see appendix - I)

$$t = r\left[\left\{1 + \frac{\rho_{Mg}}{\rho_{Ni}\left(\frac{100}{W_{Ni}} - 1\right)}\right\}^{1/3} - 1\right] \qquad (II.12)$$

where ρ_{Mg}, ρ_{Ni} are densities of nickel and magnesium respectively, W_{Ni} is the wt percentage of nickel and is the radius of the magnesium core particle.

When such a composite particle comes in contact with liquid cast iron i.e. at 1350°C, both nickel and magnesium expand. If the expansion of magnesium even before it transforms to vapour phase, is much more than that of nickel the shell might produce cracks at a few susceptible points or bursts. Later, when magnesium transforms into vapour state, these cracks might serve as pressure releasers and give rise to tiny magnesium bubbles which rise up and in the process get dissolved in the melt. If the film bursts liquid magnesium will react with liquid cast iron till it vapourises.

On the other hand, if cracks in the shell are not created during liquid magnesium expansion, magnesium will vapourize and impose tremendously high pressure on a week shell of nickel which is getting thinner and thinner from both outside and inside because of its dissolution in the molten iron

from outside and alloy formation with magnesium from inside thinner and thinner from both outside and inside because of its dissolution in the molten iron from outside and alloy formation with magnesium from inside. In such a situation the nickel shell might burst completely giving rise to a big magnesium vapour bubble which either quickly floats at the top or in the process gets dissolved in the iron. However, if the coating is not uniform which is more realistic to believe because of nonspheroidal shape of the magnesium core and nonideal fluidizing conditions during coating operation, then nickel shell might crack from some susceptible points instead of bursting completely and again give rise to tiny bubbles.

II.3.01 SPECIFICATIONS FOR MOLTEN IRON STREAM :

Selection of proper grade pig iron is very critical for nodular cast iron production by any method and the inmold process is not an exception. One has to follow general specifications given for some common elements like carbon, silicon, phosphorus, sulphur and some antispheroidizing elements like titanium, arsenic, tin, antimony, lead, bismuth and aluminium in order to get a clean liquid metal stream.

II.3.02 CARBON EQUIVALENT AND ITS EFFECT ON NODULE COUNT :

Carbon equivalent value (CEV) of a cast iron is defined in terms of its total carbon, silicon and phosphorus percentages, Since both silicon and phosphorus lower the

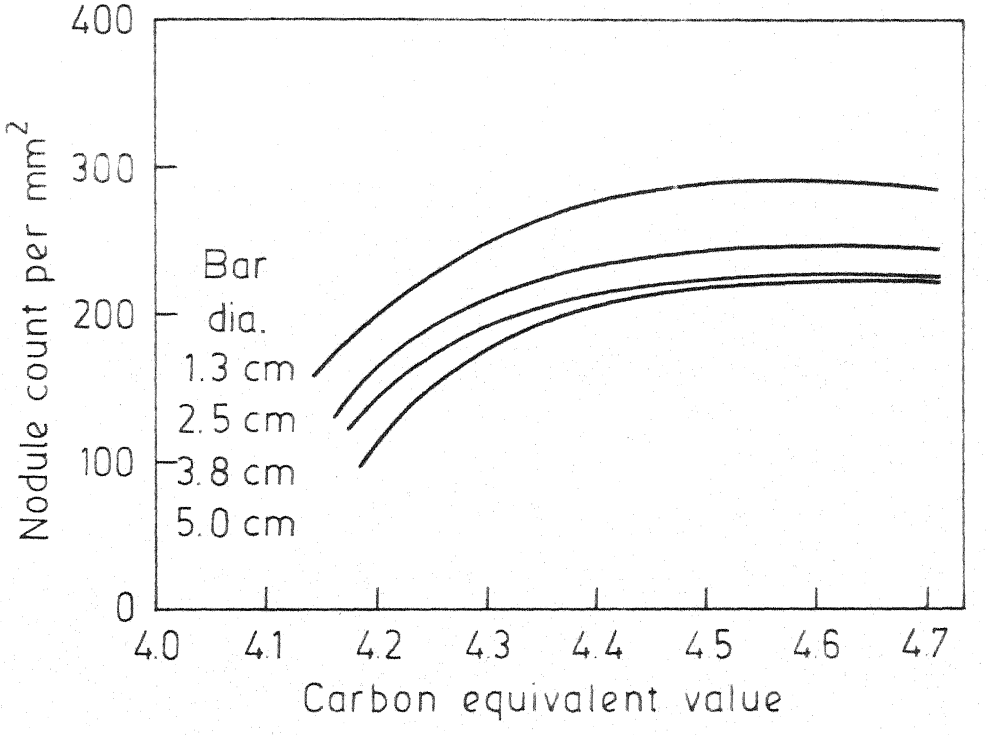

Fig. II.5. Effect of CEV on nodule count developed in a series of commercial ductile iron castings. (data from literature)

carbon content of eutectic by 0.33% for every 1% of them, the carbon equivalent value can be defined as

$$CEV = \text{Total carbon \%} + 1/3 \text{ silicon \%} + 1/3 \text{ phosphorus \%} \quad (II.13)$$

Foundry experience in the nodular cast iron production demonstrates that it is easier to form spherulitic graphite at higher carbon equivalent values. Loper[29] has obtained a graphical relationship between average values of nodule count/mm^2 and carbon equivalent value as shown in Figure-II.5

While Loper's plots show a significant increase in nodule count with increased CEV, it is to be noted that the rate of increase is much greater at the low carbon equivalent values. Loper and Nagarsheth[41] suggest that at higher carbon equivalent nodule count is insensitive to the method of inoculation. But, in general, at lower CEV the nodule count value would depend on the process.

At high CEV the problem of graphite flotation becomes significant. Since the graphite spheroid is considerably less dense than the liquid cast iron, it will tend to float when it achieves a certain size. At a constant CEV graphite flotation will then be minimized. This point is interesting from the point of view of the inmold process. Since inmold process provides more nucleation sites and thus more finer nodules, the problem of graphite flotation is obscure.

II.3.03 EFFECT OF PHOSPHORUS :

Phosphorus with iron forms steadite in nodular iron which is very brittle since the formation of steadite adversely affects toughness and ductility the wt percentage of phosphorus should not exceed 0.1 .

II.304 EFFECTS OF ANTISPHEROIDIZING ELEMENTS ON GRAPHITE SHAPE :

Thielman[30] gives an empirical quantitative expression for the combined action of antispheroidizing elements in terms of a coefficient K_1 which can be expressed by

$$K_1 = 4.4\ W_{Ti} + 2.0\ W_{As} + 2.3\ W_{sn} + 5.0\ W_{Sb} + 290\ W_{Pb} + 370\ W_{Bi} + 1.6\ W_{Al} \qquad (II.14)$$

where W_{Ti} etc represent the wt percentages of the subscripted elements.

The values of the coefficients in the equation (II.14) generally express the antispheroidizing power of the respective elements and mostly agree with the data published by other authors.

Sofroni et al.[11] define another coefficient K_2 as

$$K_2 = \frac{K_1}{W_{Mg}} \qquad (2.15)$$

where W_{Mg} is the wt per centage of the residual magnesium in the cast iron.

Figure- II.6 shows data obtained by Sofrani et al which gives a relationship between K_2 and the amount of different shapes of graphite. This plot is an attempt to delineate the zones corresponding to nodular graphite, vermicular graphite and flake graphite which are formed in zone-I, zone-II and zone-III respectively. It is also clear that nodular graphite cast iron can be obtained with the factor K_2 varying upto 8 Vermicular graphite forms if K_2 lies between 10 and 30 beyond which flake graphite will be formed. Thus equation (II.15) gives us a very convenient guideline to calculate the required residual magnesium which will provide us nodular graphite.

Loper[29] suggests that a surplus of magnesium prevents vermicular graphite formation but allows the remaining liquid to solidify as a carbide eutectic if the temperature of the liquid reaches the carbide eutectic nucleation temperature.

The influence of a number of elements on graphite shape in Fe-C-Si is summarized in Table-II.2

Gorshkov[2] points out that antispheroidizing elements have some common characteristic properties such as high specific weight, low melting point (except titanium), very high boiling point and also the capacity of decreasing the surface tension of the cast iron . Moreover they are susceptible to form chemical compounds with magnesium such as Mg_3Bi_2 , Mg_2Sn, Mg_2Pb, Mg_7n_3, MgCd etc.

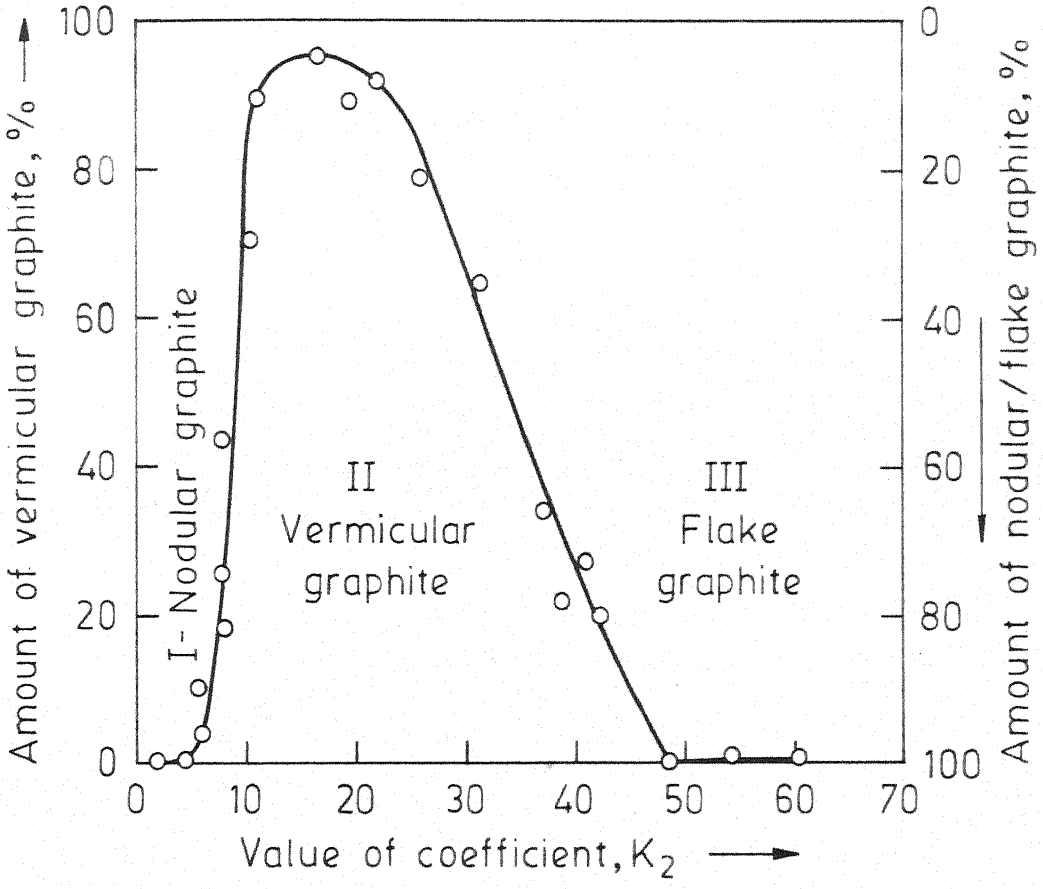

Fig. II.6. Influence of coefficient K_2 upon the amount and type of graphite.

TABLE II.2 EFFECT OF SOME ELEMENTS ON THE SHAPE OF GRAPHITE IN CAST IRON :

Spheroidizing Action				Antispheroidizing Action			
In the presence of S & O_2		In the absence of S & O_2		In the presence of S & O_2		In the absence of S & O_2	
Slow cooling	Rapid cooling	Slow cooling	Rapid cooling	Slow cooling	Rapid cooling	Slow cooling	Rapid cooling
Mg,Ca	Mg,Ca,Y	Li,Mg	Li,Na,K	Li,Na,K	Li,Na,K	Na,K	Hg,As,Sb Bi,Te
Y,La,Ce	La,Ce	Ca,Sr	Mg,Ca,Sr	Sr,Ba	Sr,Ba	Zn,Ca	
		Ba,Y	Ba,Zn	Zn,Cd	Zn,Cd	Hg,As	
		La,Ce	Cd,Al,Y	Hg,Al	Hg,Al	Sb,Bi	
		Th	La,Ce	Sn,Pb	Sn,Pb	Te	
			Th,Sn	As,Sb	As,Sb		
				Bi,Te	Bi,Te		

Table II.2 clearly shows that the action of both spheroidizing and antispheroidizing elements depends considerably on the presence of sulphur and oxygen as well as on the rate of cooling of castings . Most of the published work mentions that the sulphur content of the melt should be less than or equal to 0 .015% to obtain fully nodular structure. Normally available pig irons contain 0.04% of sulphur, therefore it becomes essential to desulphurize them before doing the inoculation treatment.

II.3.05 DESULPHURIZATION OF PIG IRON :

Removal of sulphur from molten cast iron during its passage through the cupola is possible only when it is operated under basic slag conditions. However, basic lined or lining less melting-zone cupolas are more expensive to operate and maintain than acid lined furnace. Therefore, in commercial acid cupolas only acid slag can be used and no desulphurization action can take place.

Removal of sulphur from acid cupolas using sodium carbonate was successfully conducted by Colbeck and Evans[31] in 1932. They demonstrated that about 1% (by wt) sodium carbonate can be used as an efficient ladle desulphurizing agent. Reactions taking place are :

$$Na_2CO_3 + FeS \longrightarrow Na_2S + FeO + CO_2 \qquad (II.16)$$

$$CO_2 + Fe \longrightarrow FeO + CO \qquad (II.17)$$

$$Na_2S + MnO + FeO + Na_2CO_3 \longrightarrow 2Na_2O + Mn + Fe + SO_2 + CO \qquad (II.18)$$

The amount of sulphur which can be removed from molten iron contained in a static, acid-lined ladle by addition of soda ash depends on the intimacy of contact between the metal and soda ash and also upon the original sulphur level in the iron . Various methods such as ladle injection, porous-plug ladle, shaking ladle etc. have been developed to increase the turbulance and thus the metal/slag contact area in the metal bath. Inspite of these developments only 50% to 60% of the sulphur present can be removed by this method. The reason of it can be seen from reaction (II.16) and (II.17) which are producing FeO. Increased FeO in the slag makes it acidic and the following reaction starts taking place

$$Na_2S + FeO \rightarrow Na_2O + Fes \qquad (II.19)$$

This reaction, therefore, says that after sometime the desulphurization reaction becomes reversible unless the slag formed is somehow removed or made basic using limestone chippings. Singh and Pednekar[32] report that the later additions cause excess erosion of ladle refractory.

Furthermore, equation (II.17) suggests that some of the CO_2 evolved from the soda ash is reduced by the action of the molten iron to CO and burns as carbon monoxide gas "candles" on the surface of the melt. This leads to a high dust and fumes emission.

An alternative desulphurizer which allows to avoid the disadvantages of soda ash is calcium carbide. The desulphurization reaction with CaC_2 takes place as follows

$$CaC_2 \text{ (solid)} + \quad CaS \text{(solid)} + 2C \text{ (graphite)} \qquad \text{(II.20)}$$

The free energy change of the above reaction as a function of temperature is given by[32].

$$F^o = - 85,680 + 26.57\ T^3 \qquad \text{(II.21)}$$

which shows that at the treatment temperature the reaction exothermic. Moreover, it gives a solid desulphurization product the sulphur from which is less likely to revert than the sulphur from the liquid slag in the soda ash process. It does not produce gas and hence there is no loss of desulphurizer as dust. Lastly, the formation of graphite creates a reducing atmosphere that protects the calcium carbide from atmospheric oxidation.

A few earlier kinetic studies[33-35] of this reaction have shown that the reaction rate is controlled by diffusion of sulphur either in the melt or in solid calcium sulphide. Therefore, like soda ash process, in this case also the approach to equilibrium and hence desulphurization will be facilitated by having a large reaction surface.

Various techniques have been developed to stir the melt after the calcium + carbide is added to the metal. Porous plug method[42] gives very good results but imposes highly sophisticated material requirements which are currently inadequate in our country. Shaking ladle[43] technique requires the rotation of the ladle itself and thus consumes a huge amount of power. Therefore, if the melt can be efficiently stirred with an external but cheaper stirrer tremendous amount of power can be saved. Singh and Pednekar have used a magnesite stirrer run by an electric motor to shake the metal bath. Narita et al. have designed a gas-lift mixing reactor in which gas is blown into molten pig iron from the bottom inside a cylindrical tube. With the result buoyancy of gas bubbles becomes a driving force for molten iron to rise in the tube from where it again fall through spouts on calcium carbide particles producing turbulance over them.

CHAPTER -III

DETAILS OF THE EXPERIMENTAL WORK :

III.01 GUIDELINE FOR EXPERIMENTAL WORK :

Experimental work was divided in the following parts:

(A) Desulphurization of the given pig iron.

(B) Preparation of inoculating alloy by coating nickel on pure magnesium powder by electroless plating.

(C) Inmold inoculation of the cast iron.

III.02 DESULPHURIZATION OF PIG IRON :

Two grades of pig iron were available whose compositions are shown in Table III.1

TABLE III.1 : WEIGHT PERCENTAGES OF SOME ELEMENTS IN THE AVAILABLE CAST IRON

Elements / Grade	%C	%Si	%S	%P	%Pb	%Bi	% carbon Equivalen =%C+1/3(%Si+%P)
Grade I	3.6	1.6	0.029	0.30	Not analysed	Not analysed	4.23
Grade II	3.9	2.58	0.01	0.11	0.002	could not be detected	4.79

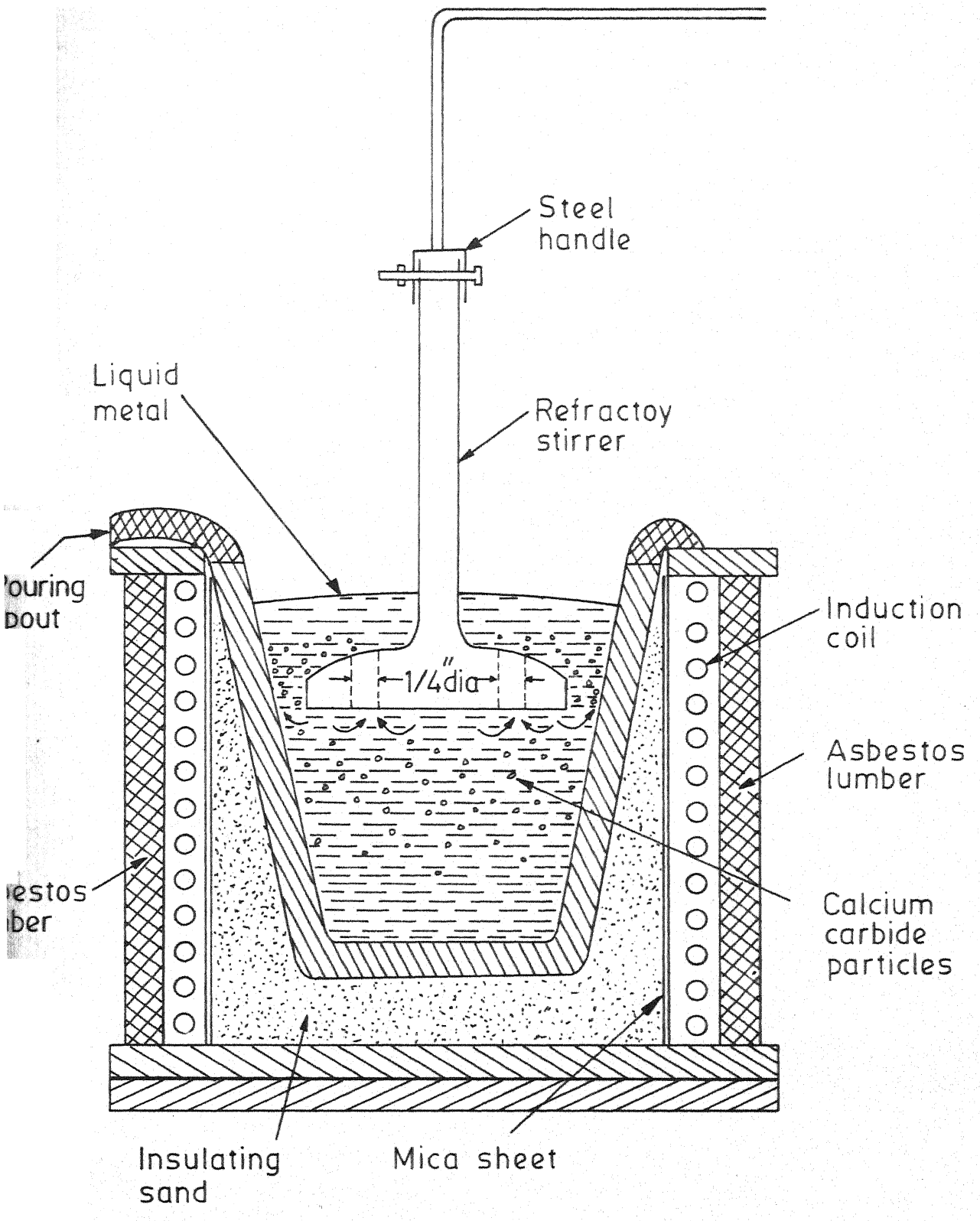

Fig. III.1. Desulphurization of pig iron.

Grade I pig iron was taken for desulphurization experiments. Commercial calcium carbide was selected as the desulphurizing agent. Its analysis was not available and it was assumed that it represented the normal grade Indian calcium carbide containing 80% CaC_2 and the rest being CaO, O, SiO_2, Al_2O_3 and MgO.[32]

Calcium carbide was available in pig lumps. It was crushed first in a steel and then in a ceramic mortar and pestle to the size distribution -200 mesh. In the process it picked up some atmospheric moisture, which was removed by dehydrating it at 110°C for 26 hours. No agglomeration of calcium carbide particles was observed during dehydration. The dehydrated calcium carbide was preserved in a dessicator with anhydrous $CaCl_2$ from picking up atmospheric moisture.

Judging from the point of view of the utility of an external stirrer, as discussed earlier in Chapter II a simple shaped stirrer, as shown in Figure III.1 was used and its performance was studied.

The stirrer was carved from a fireclay brick. As shown in the Figure III.1 it consists of two portions a horizontal disc and a handle. Diameter of the disc was kept to be 2½" so that it could easily go in the crucible containing liquid metal. Four holes of 1/4" dia were drilled on the horizontal section, two holes being on each

side of the handle (more holes can be drilled on a bigger stirrer). Upper surface of the disc was smoothened sloping downwards so that when the stirrer is pulled up the liquid metal easily slips from the top surface and fills the void created just below the stirrer.

The holes in the disc facilitate the up and down stirring motion of the stirrer and provide for added turbulance and mixing action in the liquid metal bath.

In order to melt the charge, a 1 kg clay-graphite crucible was rammed in the induction coil of a 6KW Ajax Magnethermic unit. The crucible was $2\frac{3}{4}$" deep with circular cross section and tapered side walls; its upper internal diameter being 3". Mica sheet was provided between the induction coil and crucible, and alumina powder was rammedd in between the mica sheet and coil to minimize thermal losses.

The melting charge weighed 740 gms of grade 1 pig iron. The furnace was operated at an average of KW. and it took 35 minutes to reach 1125°C, the temperature at which the charge melted. The temperature was measured by an optical pyrometer. The temperature was further raised to 1255°C . At this temperature 9.25 gms of calcium carbide (1% by wt. of the charge assuming just 80% CaC_2 in the commercial grade calcium carbide) were added to the melt. Calcium carbide powder was wrapped in a piece of paper and

then added to the metal. This avoided the loss of powder by any kind of dust emission. Stirrer was immediately put into the melt and the bath was stirred manually for 3 minutes at a rate of 30 up and down motions per minute. After that, the stirring was stopped and first batch was immediately poured in an ordinary green sand mold. No further stirring was donw and metal was poured at an interval of 2 minutes each. Moulds were of cylindrical shape, their diameters being 1". Castings were allowed to cool. Powders from each speciment were obtained by drilling operation and a wet chemical analysis for sulphur was conducted for each pouring.

IV.1.03 PREPARATION OF NICKEL COATED MAGNESIUM POWDER :

Coating of nickel, on magnesium powder was obtained using acid bath, the composition of which is given by bath-I in Table II.1. A double walled glass jacket was used to control the bath temperature which was maintained at 90 $\pm$ 1^{o}C by circulating hot oil at 95^{o}C from a constant temperature bath.

The magnesium powder taken was-325 mesh size average. It was degreased by dipping in a dilute alkali solution (10% NaOH) and was quickly rinsed with water. After degreasing it was etched by dipping in an acid solution for 10 seconds. The composition of the acid solution was

Sulphuric acid (1.84 sp.gr.)- 15% (V/V)

Water - 70% (V/V)

Chromic acid - 10 g/L

The powder was again quickly rinsed with water and water and was transferred into the hot coating bath. The bath was occasionally stirred to prevent the powder from settling. The process of coating continued for 60 minutes. The powder was taken out from the bath, rinsed and dried. It had acquired slightly darker tinge than what pure magnesium powder had. Its nickel composition was analysed by wet chemical analysis. Weight percentage of nickel was found to be 8.26 percent.

This operation was repeated on another batch of pure magnesium powder and after 60 minutes the powder was transferred to another fresh bath where it was kept for 45 minutes. Nickel in this case was found to be 11.9 percent.

TABLE III.2 DIMENSIONS OF ALLOY CHAMBERS*

Melting No.	Designation	D (inches)	2a (inches)	2b (inches)	Area (Cm^2)
1	AC-1	2.0	1	0.5	20.25
2	AC-2	2.5	1.3	0.7	31.65
3	AC-3	3.0	1.5	0.7	45.58
4	AC-4	3.5	1.75	0.9	62.04

* For '2a', '2b' and 'D' see Figure III.2

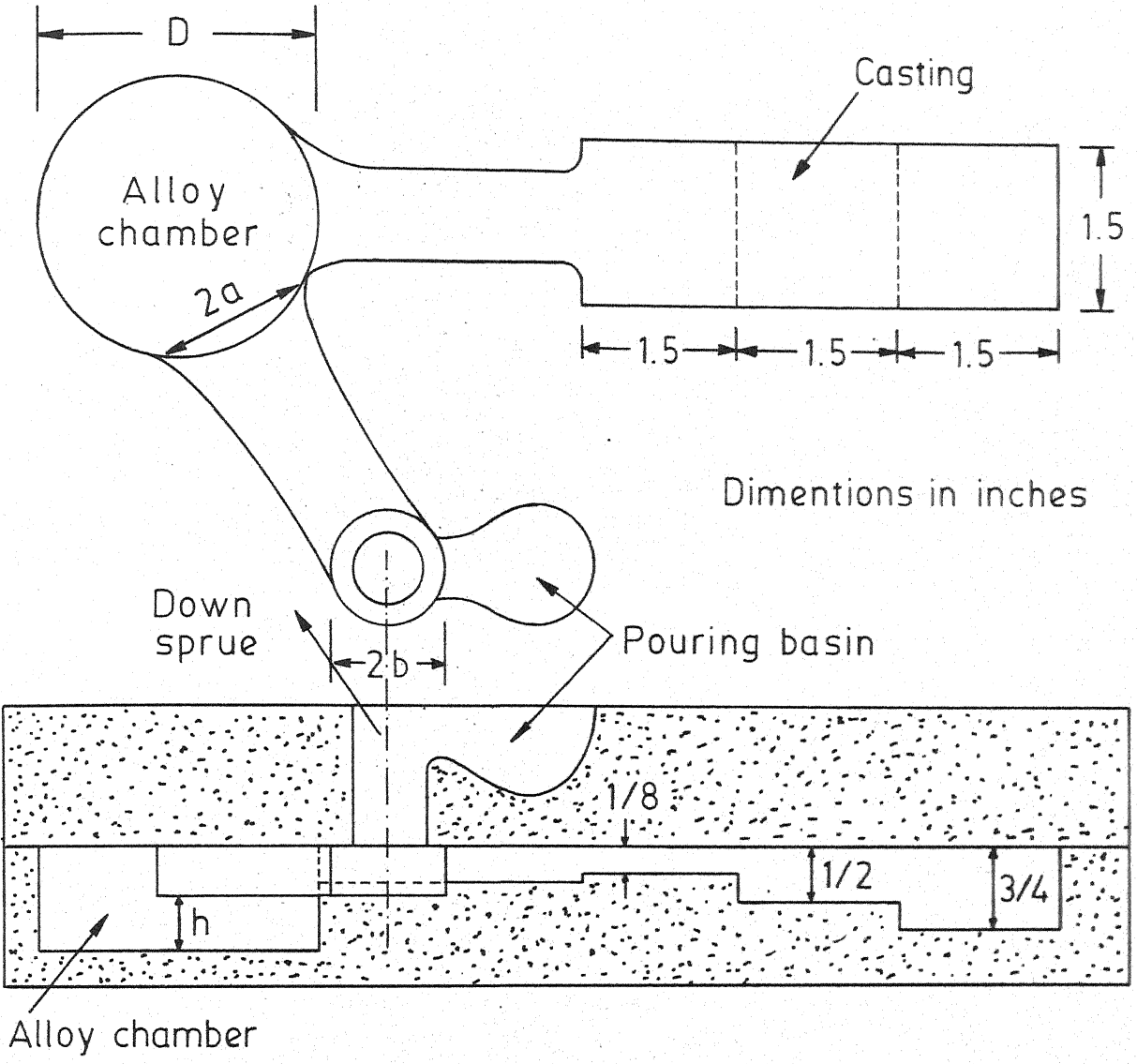

III.2. Alloy chamber scheme and the mould design.

III.04 INMOLD INOCULATION OF THE CAST IRON AND SUBSEQUENT TESTS :

The charge was melted in a 1 kg clay-graphite crucible and the source of power was a 6 kw Ajax Magnethermic induction unit.

Molds were prepared from molasses sand which was prepared by mixing about 15-18% molasses in the Yamuna sand. Molds were baked at 200°C for 1½ hr. in order to minimize the evolution of gases at the time of pouring. Shape of the molds was kept as shown in Figure II.2 and size of the alloy chamber was varied as shown in Table III.2. A pouring basin was provided and the downsprue height was kept as 1½ inches for all castings.

It was decided to use Grade II pig iron for the study of the inmold process since both sulphur and phosphorus were low in it. The charge weighed from 900 to 915 gms in each melting. No desulphurization was conducted as its sulphur content was within upper limit (0.015%). At 1350°C the melt was poured into the molds. The amount of the alloy for each run was kept as 5 gms. Castings were allowed to cool to room temperature in the mold itself.

Two reliable methods[39,40] for determining the amount of magnesium in nodular cast irons were available. The solvent extraction method suggested by Rooney and Carter[40] was preferred to that of Green[39] because the latter

is non-stoichiometric, gives a very gelatinous zinc-oxide-ferritic hydroxide precipitate and requires more amount of cast iron sample than that in the solvent extraction method. The accuracy of the solvent extraction method as given by Rooney and carter is shown in Table III.3 .

TABLE III.3 COMPARISON BETWEEN SPECTROGRAPHIC AND SOLVENT EXTRACTION METHODS FOR FINDING Mo % 40

% given by Spectrographic method	% Mo given by Solvent Extraction Method
0.017	0.018, 0.018
0.062	0.062, 0.062
0.086	0.084, 0.083
0.10	0.097, 0.10

Cast iron samples from each run were obtained by drilling out chips and were analysed by solvent extraction method (see Appendix-II for the procedure) . Microstructures were seen from each casting.

Final polishing for the microstructural examination was done on plain pellon PAD-K using diamond paste of Grade I its mean micron size being 0.5 . Pellon PAD-K is a high density, microprous, resin material of hygroscopic nature. It has not abrasive properties of its own but provides an active surface which accepts the polishing compounds in a myriad of microscopic surface voids for direct contact

with the work.

Brinell hardnews measurements were obtained at different section thicknesses of all castings.

CHAPTER- IV

RESULTS AND DISCUSSIONS

IV.01 DESULPHURIZATION OF PIG IRON :

Table IV-1 summarizes results of the desulphurization experiment.

TABLE IV-1 EFFECT OF TIME ON SULPHUR REMOVAL :

Sl.No.	Temperature (^oC)	Time after calcium carbide addition(minutes)	% S	% S Removal
1	1250	no addition	0.029	0
2	1250	3	0.0143	50.69
3	1240	5	0.0095	67.24
4	1250	7	0.0089	69.31
5	1250	9	0.009	68.96

Amount of sulphur in the pig iron and the percentage of sulphur removal as functions of time have been separately plotted in Figure IV.1 and IV.2, respectively.

It is seen from these plots that the desulphurization continues even after the external stirring is stopped (3 minutes after calcium carbide addition). In fact, 25-28% of the total sulphur removed is desulphurized after the refractory stirrer is withdrawn.

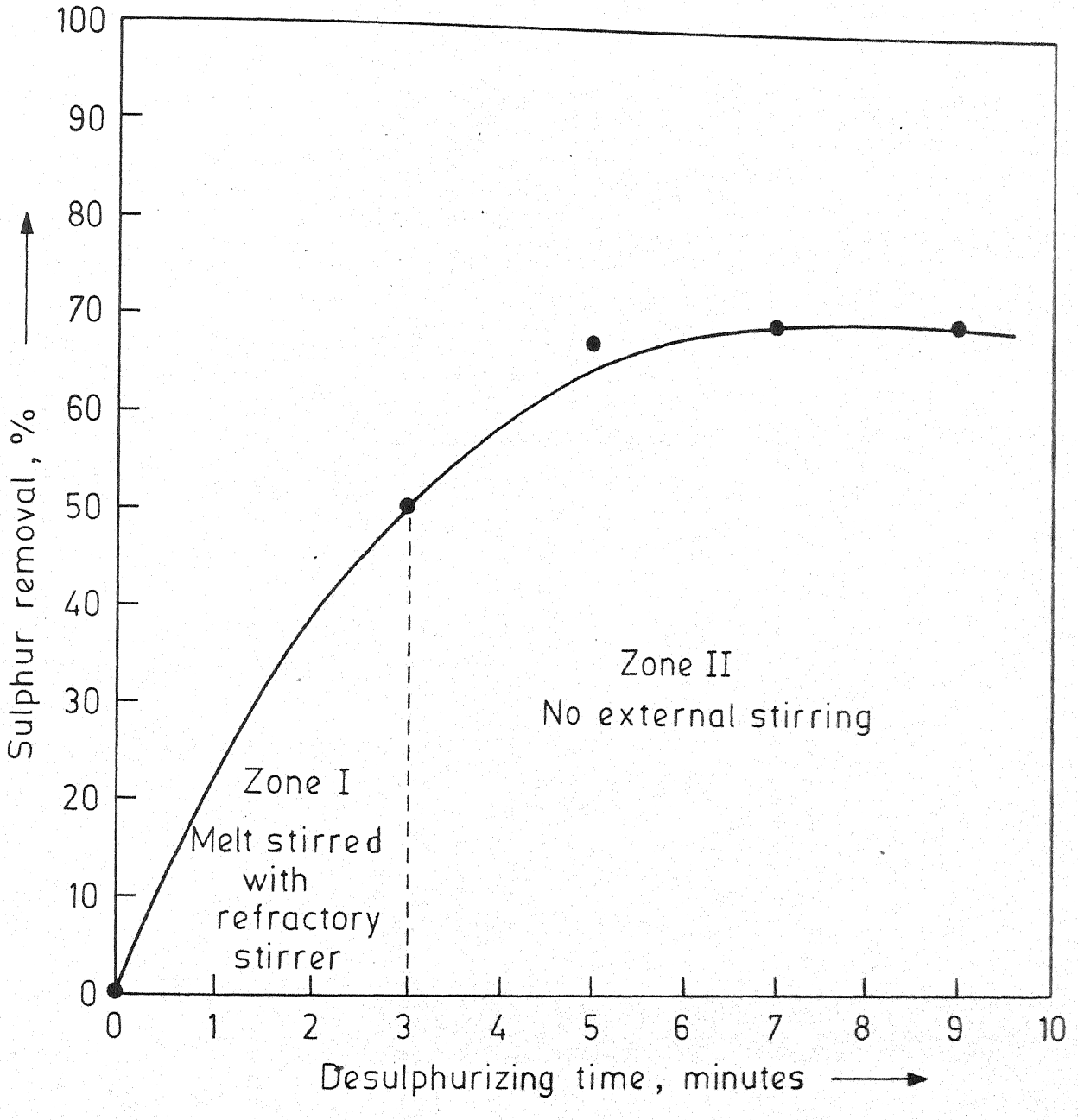

Fig. IV. 2. Percentage sulphur removal as a function of desulphurization time at the treatment temperature of 1255°C.

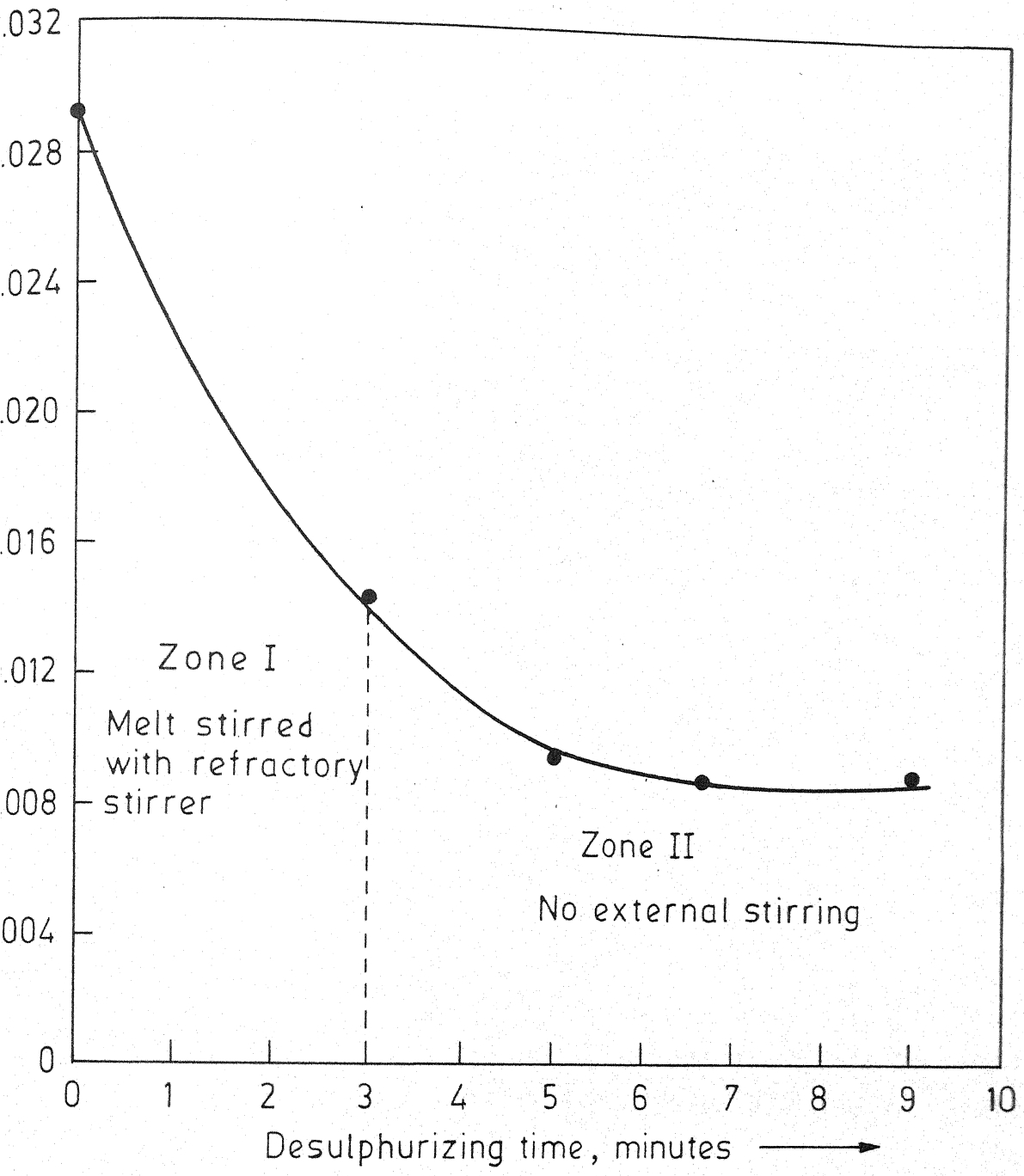

IV.1. Sulphur content as a function of desulphurization time at the treatment temperature of 1255°C.

A probable reason for the continued desulphurization might be the internal stirring produced by eddy currents generated in the melt by induction coil. This internal stirring keeps the concentration of sulphur at the calcium sulphide/melt interface (due to desulphurization calcium sulphide is formed on each calcium carbide particle) same as that in the bulk and thus helps in continuing desulphurization before particles rise at the top and loose their contact with the liquid metal. Apart from the stirring created by eddy currents, each particle, due to its vertical movement in the melt, exposes itself to a fresh sulphur rich melt and thus assists in continued desulphurization.

Results plotted in the figure also indicate that the sulphur content required for nodular cast iron production (0.015%) is obtained from the given grade of pig iron within 3 minutes after calcium carbide addition and melt stirring. However, more time for desulphurization will be preferred because lower sulphur, which is possible by the method helps in increasing magnesium recovery and decreasing possibilities of MgS inclusions in the casting.

Removal of sulphur stopped at 0.009% and was about 70% of the initial sulphur present in the pig iron. Percentage removal of sulphur is expected to be higher for high original sulphur.

The fireclay stirrer, at the laboratory scale worked as a satisfactory stirrer and lasted for 3 to 5 heats before its erosion.

IV. 0.2 INMOLD INOCULATION OF CAST IRON AND SUBSEQUENT TESTS :

6 Kw Ajax Magnethermic induction unit was used for the melting. The charge was melted in a 1 kg clay graphite crucible. Amount of charge per melting was kept from 900 to 915 gms.

The variables which can be considered in the inmold process are :

(1) Velocity of the metal stream when it passes over the inoculating alloy in the alloy chamber.
(2) Horizontal cross section of the alloy chamber.
(3) Treatment temperature.
(4) Composition of the inoculating alloy.
(5) Section thickness of the casting (which is a variable for all other methods of nodular iron production also).

Since McCaualy suggests that the value of the solution factor does not vary much with the temperature and remains constant for $\pm$ 40 ^{o}C, the treatment temperature, in this study was kept constant at 1350 ^{o}C.

Variables considered in this study were alloy chamber area and section thickness of the casting. Since the velocity of metal stream is function of its free fall,

a pouring basin was provided and downsprue height was kept as $1\frac{1}{2}$ inches for all runs.

Table IV-2 summarizes results of magnesium analysis by solvent extraction method (see Appendix II).

TABLE IV.2 PERCENTAGE OF MAGNESIUM IN CASTINGS OF DIFFERENT ALLOY CHAMBER AREAS :

Melting No.	Amount of sample analysed (gms)	Vol. of 0.01M E.D.T.A.* (ml)	% Mg	Area of the alloy chamber (cm^2)
M_1	10	5.3	0.0129	20.25
M_1	10	5.5	0.0134	20.25
	10	6.1	0.0149	
M_2	10	6.4	0.0156	31.65
	10	6.3	0.0154	
M_3	5	5.3	0.0259	45.58
	5	5.5	0.0268	
M_4	55	6.5	0.0318	62.04
	5	6.4	0.0313	

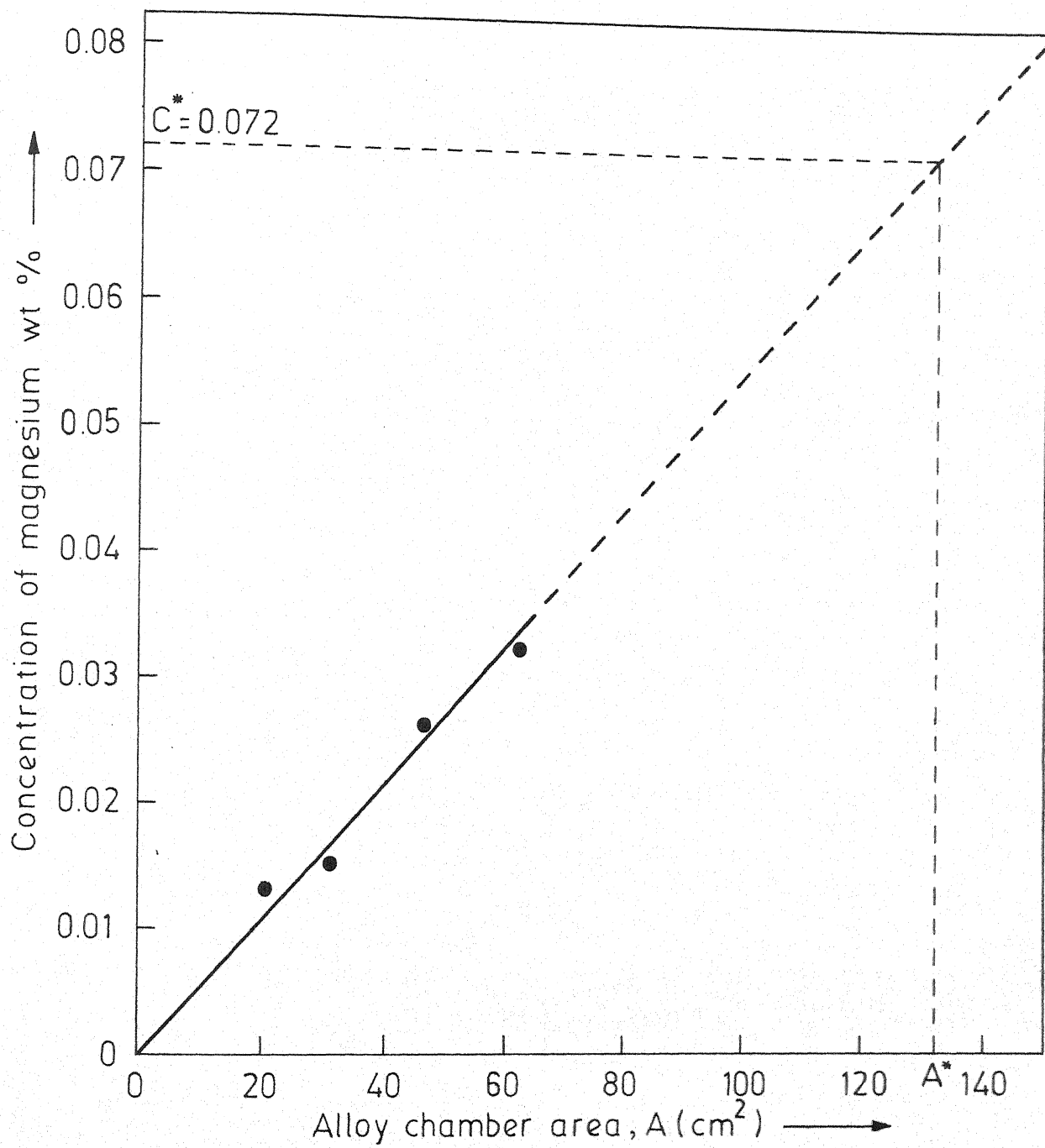

Fig. IV. 3. Area concentration curve (ACC) for nickel coated magnesium powder at the treatment temperature of 1350°C.

The optimum quantity of the residual magnesium is, therefore, approximately 0.07%.

CALCULATION OF THE SOLUTION FACTOR :

Solution factor is the optimum ratio between the metal stream velocity and the alloy chamber area. The average velocity of the metal stream which was kept over all alloy chambers was 25 cm/sec (see Appendix III). From figure IV.3, the optimum alloy chamber area, A* was obtained which was found to be 130 cm^2 . Therefore,

$$\text{Solution factor , } f = \frac{V_{av}}{A^*}$$

$$= \frac{25 \text{ cm/sec}}{130 \text{ cm}^2}$$

$$= 0.19 \text{ cm}^{-1} \text{ sec}^{-1}$$

PERCENTAGE ALLOY RECOVERY :

Table IV.3 gives the percentage alloy recovery in different castings. Alloy recovery has been computed two times, first on the basis of the weight of the step shape casting (390 gms) in the fourth column and again on the basis of the total inoculated iron including the alloy chamber in the column six .

TABLE IV.3 PERCENTAGE ALLOY RECOVERIES

Meeting No.	Alloy Chamber Area (cm^2)	%Mg	% Alloy Recovery on the basis of the step casting wt (390 gms)	Wt. of the casting including that of the alloy chamber(gms)	% Alloy recover of the basis o the wt. total i culated iron
1 M_1	20.25	.013	1%	582	1.5%
2 M_2	31.65	.015	1.19%	660	2.0%
M_3	45.58	.026	2.0%	760	4.0%
M_4	62.00	.032	2.5%	875	5.7%

It should be noted that alloy recovereies reported in Table IV.3 are in no way representatives of those obtained in actual inmold process. The reason for extremely low alloy recovery is that in order to study the effect of a particular alloy chamber area one has to keep a fixed quantity of alloy even if the casting weight does not require it. The extra alloy, which remains in the alloy chamber after the stream fills the actual casting does not find any opportunity to be dissolved and leads to a poor recovery. However, if the casting is big enough, most of the alloy will be consumed by the flowing metal stream and recovery will be quite high.

However, it is clear from the above data that the increase in alloy chamber area is providing improved inoculant recovery.

MICROSTRUCTURES :

Table IV 4 gives the value of coefficient K_2, computed from equation II.15 and the types of expected and actually observed microstructures.

Table IV.4 Prediction of microstructure from the residual magnesium content

Melting No.	Residual Magnesium content (%)	K_2	Type of microstructure predicted from Fig. II.6	Type of microstructure actually observed.
M_1	0.013	44.6	Flake	Predominantly flake
M_2	0.015	38.6	Flake + Vermicular	Flake + Vermicular
M_3	0.026	22.3	Vermicular	Flake + Vermicular
M_4	0.032	18.1	Vermicular	Flake + Vermicular

Microstructures at the section thickness of 3/4 inch are shown in Figure IV. 4. It is seen that in all cases microstructures can be considered as mixtures of both flake and vermicular graphite. This observation is slightly different than that of sofrani et al.[11] who predict that at least in meltings M_3 and M_4 we should get almost 100% vermicular graphite. This difference, however, is understandable because transition limits defined by sofroni et al. have been obtained after an oversimplification of the process and thus are subjected to minor adjustments.

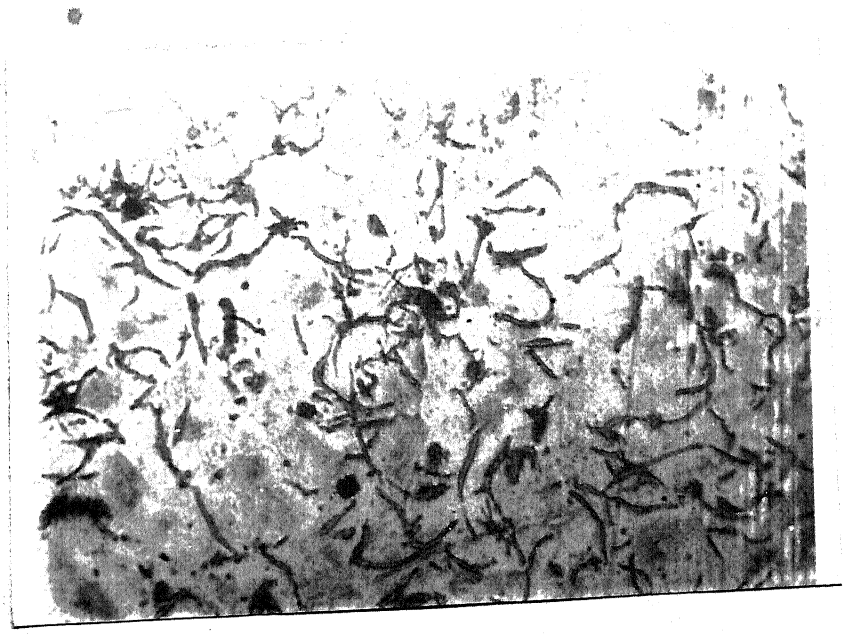

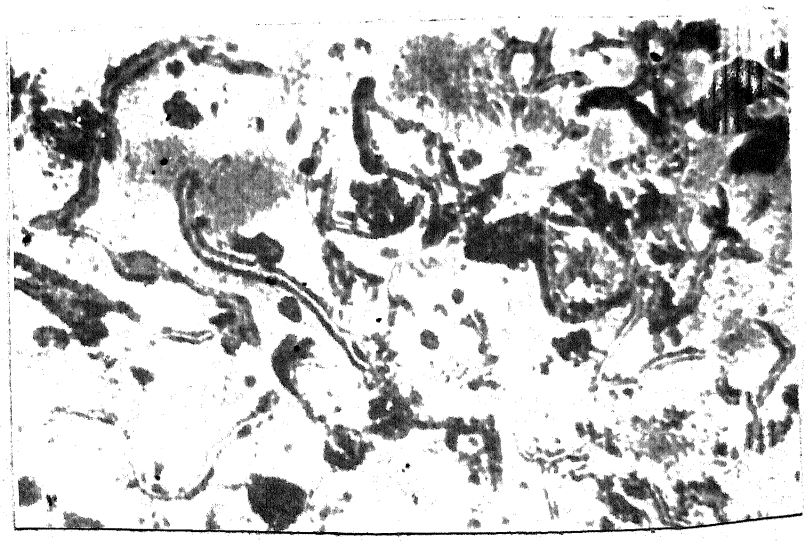

HARDNESS :

Table IV.5 gives the Brinell Hardness number for castings at section thicknesses of 3/4 inch and 1/2 inch.

Table IV.5 Brinell Hardness Measurement

Load applied = 3000 Kg.

Ball diameter = 10 mm

Indentation time = 15 sec.

Section thickness (inch.)	Melting 1 K_2 = 44.6		Melting 2 K_2 = 38.6		Melting 3 K_2 = 22.3		Melting 4 K_2 = 18.1	
	Dia. (mm)	BHN	Dia (mm)	BHN	Dia (mm)	BHN	Dia (mm)	BHN
3/4	4.1	217	4.15	212	4.75	159	5.7	107
	4.15	212	4.15	212	4.75 4.70	159 163	5.65	109
	3.95	235	4.0	229	4.40	187	4.9	149
1/2	3.95 3.90	235 241	4.05	223	4.45	183	4.95	146

Figure IV.5 shows the plot between BHN and the coefficient K_2. It can be seen that the region in the plot can be distinctively divided into two zones. While in zone- I, the rate of increase in hardness with K_2 is much steep, it is extremely low in the zone-II. A probable reason for this observation lies in the fact that zone-I is the region where microstructure is changing from complete flake to complete

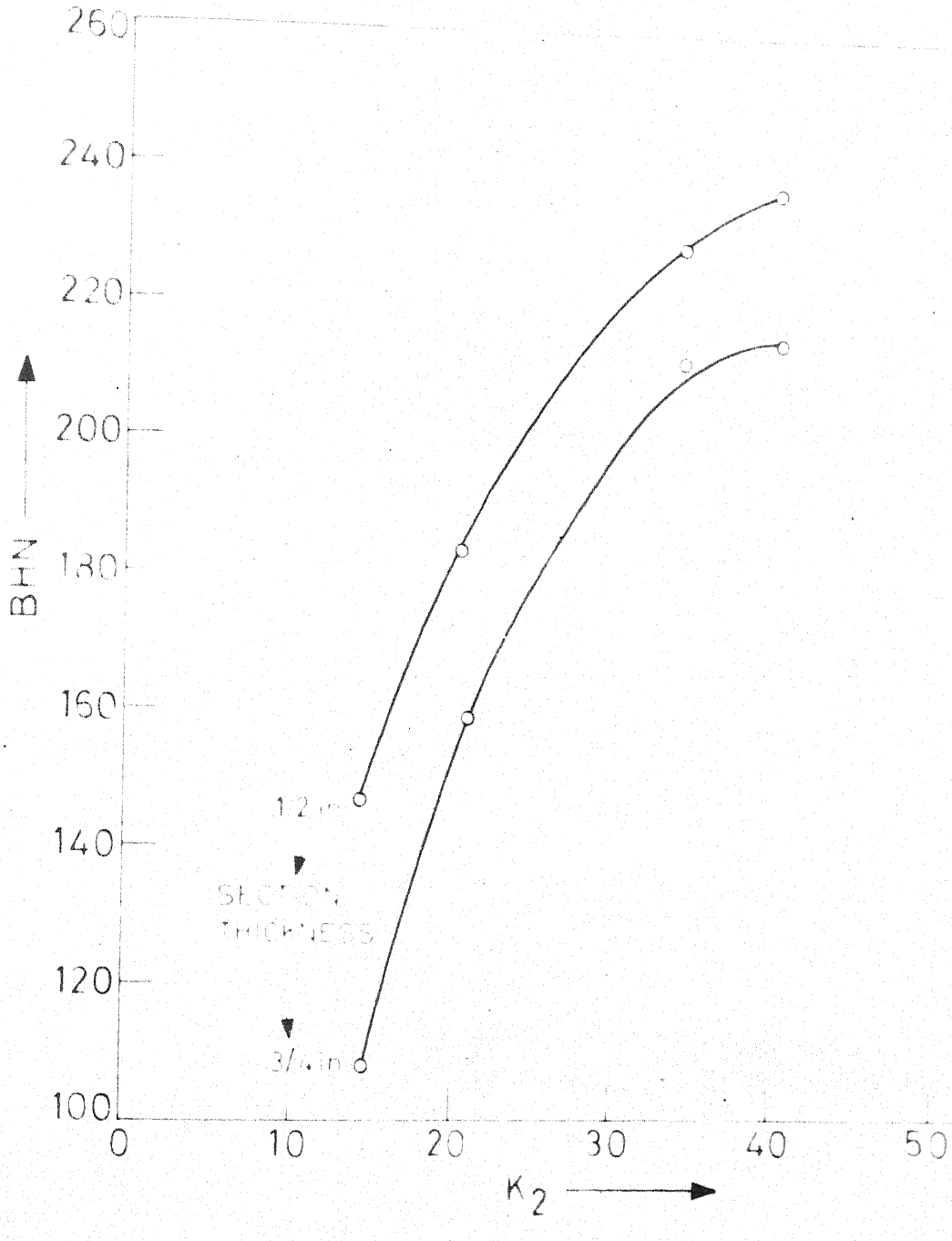

Fig IV.5 Effect of K_2 on the hardness value

vermicular and since the amount of each type of graphite depends on K_2 , the change in any mechanical property in this region will be very sensitive to K_2 . However, to strengthen the above statement one would require more experimental data.

CHAPTER V

CONCLUSIONS

The following conclusions can be drawn from the presented work.

(a) Desulphurization with 1% calcium carbide addition, required for nodular iron production, is possible by stirring the melt with a simple shaped refractory stirrer.

(b) Solution factor of a -325 mesh nickel coated magnesium powder (11.9% nickel coated by electroless plating) is found to be 0.2 cm^{-1} sec^{-1} for the given pig iron at the pouring temperature of 1350°C.

REFERENCES

1. Yamamoto, S. et.al., Metal Science, Vol.9, (1975), p.360-369.
2. Gorshkov, A.A., Corresponding Member, Authors certificate No. 110353.
3. Morrogh, H. and Williams, W.J., JISI, Vol. 158, (1948) p.306-322.
4. Erich K. Modl., Foundry, Vol. 98, (1970), p.42-48.
5. Morrogh, H, Journal of Research and Development (BCIRA), Vol. 5, No. 12, (1955), p.655-671.
6. McSwain, R.H., and Bates, C.E., "Metallurgy of cast Iron" edited by Lux, B., Georgi Publishing Co., Switzerland, (1974), p.423-442.
7. Buhr, R.K., Modern Casting, Vol. 54, (1968) p.497-503.
8. Double, D.D. and Hellawell, A., "Metallurgy of Cast Iron" edited by Lux, B. Georgi Publishing Co., Switzerland, (1974), p.509-528.
9. Backerud, L., Nilsoon, K., and Steen, H., ibid, p.625-637.
10. Loper, C.R., Jr., Heine, R.W., Chaudhri, M.D., ibid, p.639-657.
11. Sofroni, L., Riposan, I. and Chira, I., ibid,p.179-195.
12. Remondino, M. et al., ibid, p.163-178 .

13. Remondino, M. et al., International Cast Metal Journal, Vol. 1, (1976) p.30-52.

14. Dunks, C.M., Hobman, G., and Mannion, G., Modern Casting, Vol. 64, (1974) p.48.

15. McCaulay, J.L., Foundry Trade Journal, Vol. 130 No. 2836, (1971), p.327-335.

16. Hillner, G. Fr., Kleemann, K.H., Thexton, T.J., Foundry Trade Journal, Vol. 141, No. 3092, (1976) p.297-310.

17. Moore, Wm.H., Modern Casting, Vol. 63, No. 3, (1973) p.37-39.

18. Mannion, G., Modern Casting, Vol. 101, No. 1, (1973) p.80-84.

19. Smallev, O., Foundry Trade Journal, Vol. 139, No. 3068, (1975) p. 423-430.

20. Peregulov, L.V. et al., Russion casting Production,

21. Ryntz, E.F., and Arnson, H.L., Modern Casting, Vol. 66, No. 1, (1976), p.53-54.

22. Schleg, Fred P., Modern Casting, Vol. 65, No. 10, (1975), p.46-47.

23. Annonymous, Foundry, Vol. 102, No. 4, (1974) p.68-70.

24. Moore William, H. Patent No. U.S.3, 765,876 (Cl 75/130A; C22C) 16 Oct. 1973, Appl. 302, 762, 01 Nov. 1972, 8pp.

25. Karasay, Stephen, I., Foundry, Vol. 100, No. 8, (1972), p.41-43.

26. Rao, B.V., Rao, Y.V., Saha, R.L., and Tambankar, R.V., Transactions of the Indian Institute of Metals,

27. Kaul, R.K., I.I.T. Kanpur, M. Tech. Thesis Department of Met. Engg., Jan. (1975).

28. Bremer, A., Riddell, G.E., Proceedings American Electroplaters Soc., Vol. 34, (1947), p.156.

29. Loper, C.R., Modern Casting, Vol. 55, No. 1, (1969), p.1-7.

30. Thiehman, Th, Giessereitechnik, No. 1, (1970)p.16-24.

31. Evans, N.L., Foundry Trade Journal, 1-22 Dec. and 5 Jan. 1932-3 .

32. Singh, R.P. and Pednekar, S.P., Trans. Indian Institute of Metals, Vol. 29, No. 2, (1976), p.140-143.

33. Hitchcock, P.A., Mitchell, A., JISI, Vol. 204, No. 3, (1966), p.226-229.

34. Ooi, H. et al, Trans. ISI Japan, Vol. 12, (1972), p.1-5.

35. Ando, R., and Fukushima, T., Trans, ISI Japan, Vol. 1, (1971), p.179-183.

36. Khropov, A., and Bedarev, V.J., Russian Casting Production, (1963), p.164-7.

37. White, R.W., Foundry Trade Journal, Vol. 116, (1964), p.164.

38. Gorshkov, A. and Rudenko, N.G., " Gaes in Cast Metals" edited by Gulyaev, B.B. consultants Bureou, New York (1965), p.77-82 .

39. Green, H., BCIRA Journal of Research and Development, Vol. 6, No. 1, (1955), p.20-22 .

40. Rooney, R.C. and Carter, Beryl., BCIRA Journal of Research and Development.

41. Loper, C.R. Jr., Jagarsheth, P.S. and Heine, R.W. Gray Iron News, June 1964, p. 5-17 .

42. Narita1, K. et al, Trans. ISIJ, Vol. 16 (1976) p 504- 512 .

APPENDIX I

CALCULATION OF THE NICKEL SHELL THICKNESS OVER A CORE PARTICLE OF MAGNESIUM :

Let r and R be the rodii of pure magnesium particle and magnesium nickel composite respectively. Assuming ρ_{Mg} and ρ_{Ni} to be densities of pure magnesium and pure nickel, the weight percentage of nickel will

$$W_{Ni} = \frac{4/3\,\pi\,(R^3 - r^3)\,\rho_{Ni}}{4/3\,\pi\left[(R^3 - r^3)\,\rho_{Ni} + r^3\,\rho_{Mg}\right]} \times 100$$

$$\text{or} \quad 1/W_{Ni} = 0.01 \left[\frac{(R^3 - r^3)\,\rho_{Ni} + r^3\,\rho_{Mg}}{(R^3 - r^3)\,\rho_{Ni}} \right]$$

$$= 0.01 \left[1 + \frac{r^3}{(R^3 - r^3)} \cdot \frac{\rho_{Mg}}{\rho_{Ni}} \right]$$

$$\text{or} \quad (100/W_{Ni} - 1)\,\frac{\rho_{Ni}}{\rho_{Mg}} = \frac{r^3}{(R^3 - r^3)}$$

$$\text{or} \quad \frac{R^3 - r^3}{r^3} = \frac{\rho_{Mg}}{\rho_{Ni}\,(100/W_{Ni} - 1)}$$

$$R/r = \left[\left(1 + \frac{\rho_{Mg}}{\rho_{Ni}\,(100/W_{Ni})} - 1 \right) \right]^{1/3}$$

Therefore the shellthickness $t = R - r$

$$= r \left[\left\{ 1 + \frac{\rho_{Mg}}{\rho_{Ni}\,(100/W_{Ni}) - 1} \right\}^{1/3} - 1 \right]$$

APPENDIX II

SOLVENT EXTRACTION METHOD FOR THE DETERMINATION OF MAGNESIUM IN THE NODULAR CAST IRON[40]

PREPARATION OF REAGENTS AND SOLUTIONS :

1. E.D.T.A. Solution : 3.72 gms of disodium ethylene diaminetetra-acetate dihydrate was dissolved in water and the solution was diluted to 1 liter.
2. Erichrome Black-I indicator : 0.1 gm of Erichrowe Black-I was dissolved in 100 ml. of 30:70 triethanolamine.
3. Ammonium hydroxide-Ammonium chloride Buffer Solution: 67.5 gms of ammonium chloride was dissolved in a mixture of 570 ml. of ammonoum hydroxide, and 300 ml. of water and was diluted to 1 litre.
4. Sodium Diethyldithiocarbomate: Only freshly prepared solution was used. Solution was prepared by adding 200 g.p.l. sodium diethyldithiocarbamate in water.
5. Sodium Acetate, 2M : 272 gms of sodium acetate trihydrate were dissolved in water and the solution was diluted to 1 litre.
6. Cupferron: Only freshly prepared solution was used which was prepared by adding 600 g.p.l. of cupferron in water.

PROCEDURE : For meltings M-1 and M-2 10 gms of cast iron sample was taken. For meltings M-3 and M-4, samples weighed 5 gms each cast iron sample was taken in a squat beaker and was cautiously dissolved in a mixture of 50 ml. of hydrochloric acid and 15 ml. of nitric acid. When the sample was dissolved completely it was filtered into a 250 ml. conical separating funnel using a glass wool pad. Beaker and pad were washed three times with hydrochloric acid. 150 ml of iso-butyl acetate were added and the solution was shaken vigorously and was given sufficient time so that two phases could separate.

The lower (acid) layer was run into a 400 ml, squat beaker, allowing the interface to travel at the bottom of the stopcock bore and the inside of the funnel stem was rinsed with water. 150 ml. of perchloric acid was added and the solution was evaporated to fumes.

After 3-5 minutes, 25 ml. of water were added and the solution was heated to boiling after which it was filtered on a paper pulp pad into 250 ml. conical separating funnel. Separating funnel was cooled and 50 ml. of 2M sodium acetate solution were added to it. 10 ml. of cupferron solution, 30 ml. of chloroform were also added and the solution was shaken vigorously. Two phases were allowed to separate and the lower layer was run off. 40 ml. of sodium diethylithiocarbamate solution and 50 ml. of chloroform were

added to the aqueous layer in the funnel and the solution was again vigorously shaken. Two phases were allowed to separate and the lower layer was run off. Stopper and the neck of the funnel were rinsed with chloroform.

10 10 ml. of chloroform and 1-2 ml. of sodium diethyldithis carbamate were further added to the solution and a white precipitate was obtained. Solution and a shaken to extract the precipitate into the chloroform and was allow to separate. Chloroform layer was run off. This procedure was repeated till the chloroform layer became colourless. Before running off the last layer of chloroform 2-3 drops of cupferron were added. A coloured precipitate was obtained. Cupferron was added till this precipitate became white. More chloroform was added to extract this precipitate and the chloroform layer was separated.

Aqueous layer of the solution was to a 400 ml. beaker and 15 ml. of ammonia-ammonium chloride buffer solution and 10 drops of Erichrome Black-I indicater were added. The solution was titrated with 0.01M of E.D.T.A. untill the colour of the solution changed from pink through purple to a pure blue end point.

The amount of magnesium was calculated from

1 ml. of 0.01M EDTA $\equiv$ 0.2432mg of Mg

$\equiv$ 0.0049% Mg on 5gm sample

APPENDIX III

CALCULATION OF THE AVERAGE VELOCITY OF THE LIQUID METAL STREAM OVER THE ALLOY CHAMBER AREA :

Figure-A III shows the top view of an alloy chamber of radius R with its inlet and outlet at its left and right respectively. Assume that the metal after falling through the downsprue of height H hits the runner at plane (1) which has a width of 2b as shown in the figure . Let 2a and 2c be the widths of the runner system at inlet and outlet respectively.

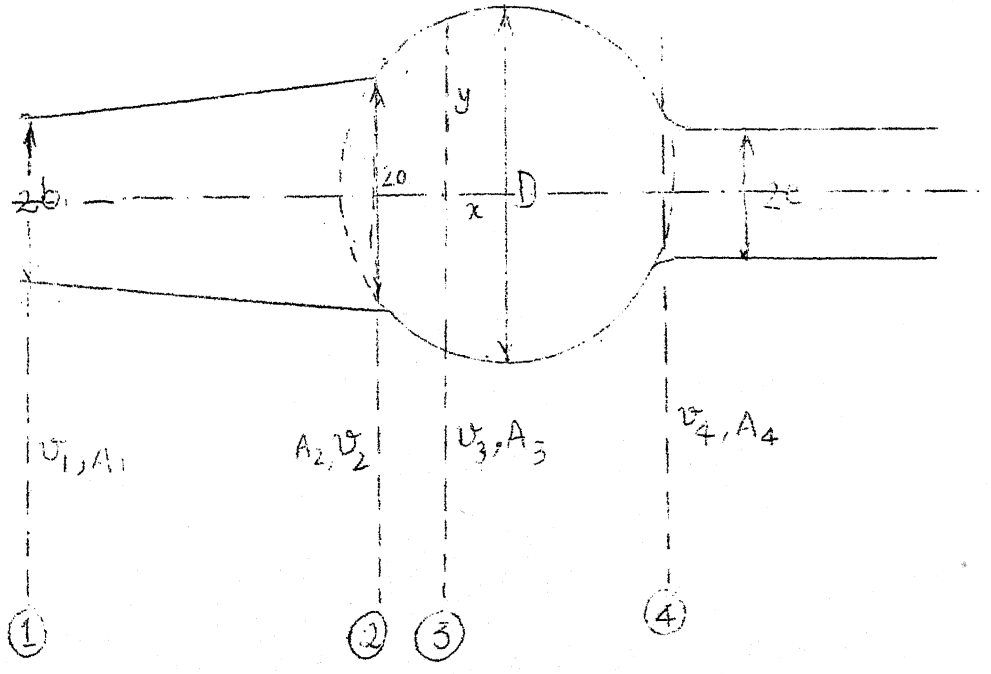

Figure - A III

Velocity of the metal at the bottom of the sprue will be

$$v_1 = 2gH \qquad \text{(III a)}$$

Applying continuity equation on planes (1) and (2), we obtain that

$$v_1 2bh = v_2 2ah \qquad \text{(IIIb)}$$

or $v_2 = v_1 b/a$

or $v_2 = (b/a)\ 2gH \qquad \text{(III c)}$

In our case, $h = 1\frac{1}{2}$ in, b/a 1/2

Therefore

v_2 = 1/2 2 x 32 x 12 x(3/2) in/sec

17 in/sec

40 cm/sec

From the above calculation we see that the velocity of the liquid stream is sufficiently low and hence bend losses in the runner system can be assumed to be zero and the flow can be considered to be in a straight line as shown in the figure.

When the liquid metal enters the alloy chamber its velocity decreases as the cross sectional area of the stream increases, reaching a minimum when cross sectional area is maximum and again decreases.

Applying continuity equation at planes (2) and (3) we get

$$2ahv_2 = 2yhv_3$$

or $$v_3 = av_2/y$$

or $$v_3 = av_2/\sqrt{(R^2 - x^2)} \qquad \text{(III d)}$$

Therefore, in the region I, the average velocity is

$$v^1_{av} = \frac{1}{\sqrt{(R^2 - a^2)}} \int_0^{\sqrt{(R^2 - a^2)}} \frac{av_2\, dx}{\sqrt{(R^2 - x^2)}} \qquad \text{(III f)}^*$$

$$\text{or} \quad v^1_{av} = \frac{av_2}{\sqrt{(R^2 - a^2)}} \left[\text{Sin}^{-1} \frac{x}{R} \right]_0^{R^2 - a^2}$$

$$= \frac{v_2}{\sqrt{(R/a)^2 - 1}} \left[\sin^{-1} \sqrt{1 - \left(\frac{a}{R}\right)^2} - \sin^{-1}(0) \right]$$

$$\text{or} \quad v^1_{av} = \frac{v_2 \sin^{-1} \sqrt{1 - (a/R)^2}}{\sqrt{(R/a)^2 - 1}} \qquad \text{(III g)}$$

Similary, $$v^{II}_{av} = \frac{v_4}{\sqrt{(R/C)^2 - 1}} \sin^{-1} \sqrt{1 - (c/R)^2}$$

---

* average of a function $y = f(x)$ between $x = a$ and $x = b$ is given by

$$y_{av} = \frac{1}{b - a} \int_a^b f(x)\, dx$$

In our experiment $a \simeq c$

$$v_{av}^{I,II} = \frac{v_2}{\sqrt{(R/a)^2 - 1}} \sin^{-1} \sqrt{1 - (a/R)^2}$$

In our case $R/a \simeq 2$

Therefore,

$$v_{av}^{I,II} = \frac{40}{\sqrt{(4 - 1)}} \sin^{-1} \sqrt{\left(1 - \frac{1}{4}\right)}$$

$$= \frac{40}{\sqrt{3}} \sin^{-1} (3/2)$$

$$= \frac{40}{\sqrt{3}} \cdot \frac{\pi}{3}$$

25 cm/sec.